In the cancer cell line panel, the mRNA expression levels of *FOXQ1* were higher in gastric cancer, CRC, and lung cancer cell lines than in the other cancer cell lines, indicating that the expression of *FOXQ1* varies among specific cancers (Fig. 1C, right). Interestingly, the overexpression of *FOXQ1* in CRC arose from normal colonic mucosa with very low expression levels during carcinogenesis.

p21 is a target gene of FOXQ1. To examine the function of FOXQ1 as a transcription factor and to explore its target genes, we performed a microarray analysis using a CRC cell line, DLD-1, transfected with FOXQ1-targeting siRNA or control siRNA. Two sequences of FOXQ1-siRNA, FQ#1 and FQ#4, were used to exclude the off-target effect of siRNA. Real-time RT-PCR showed that both sequences of FOXQ1-siRNA suppressed *FOXQ1* mRNA expression by ~80% in DLD-1 cells (Fig. 2A); thus, FQ#4 was used as the FOXQ1-siRNA in the following experiments. A microarray analysis showed that 19 genes were downregulated by FOXQ1-siRNA (Fig. 2B; Supplementary Table S2); *p21* was the fifth most-downregulated gene. Because p21 is a key regulator of cell cycle and apoptosis, we focused on p21 as a target molecule of FOXQ1.

To confirm the microarray data, p21 downregulation by FOXQ1-siRNA was examined using real-time RT-PCR and a

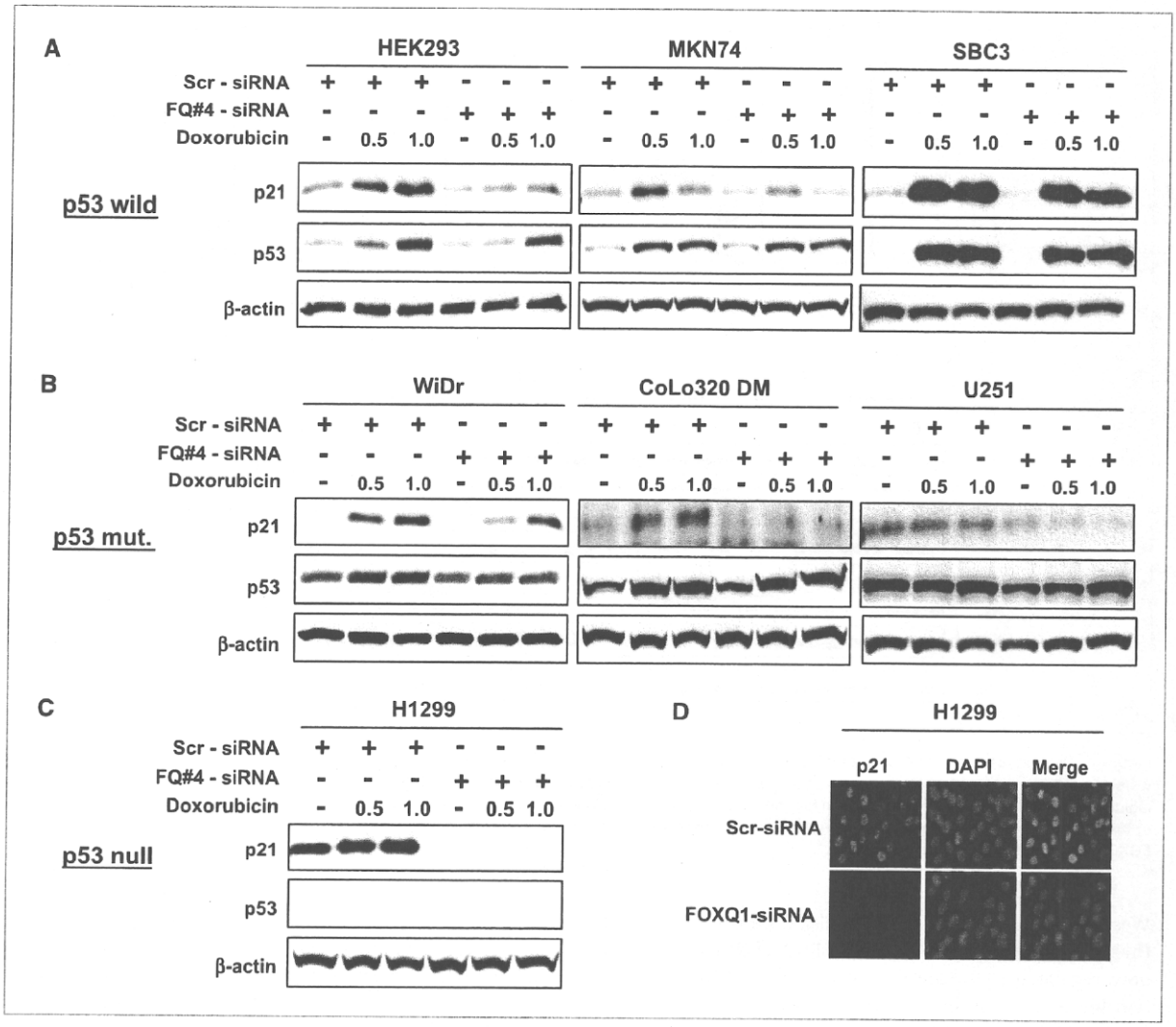

Figure 3. p21 induction by FOXQ1 and p53 status in cancer cells. The seven cell lines were transfected with control-siRNA or FOXQ1-siRNA for 24 h, and the cells were exposed to doxorubicin at a final concentration of 0.5 or 1 μmol/L for a further 24 h to enhance p21 induction. Western blot analyses for p21 and p53 were performed in three p53–wild type cell lines (A), three p53-mutant cell lines (B), and one p53-null cell line (C). The experiment was performed in duplicate. D, immunofluorescence p21 staining and 4′,6-diamidino-2-phenylindole (DAPI) staining for H1299 cells transfected with control-siRNA (top) or FOXQ1-siRNA (bottom) for 48 h. Scr, scramble-siRNA (control); FQ#4, FOXQ1-targeting siRNA. β-Actin was used as an internal control.

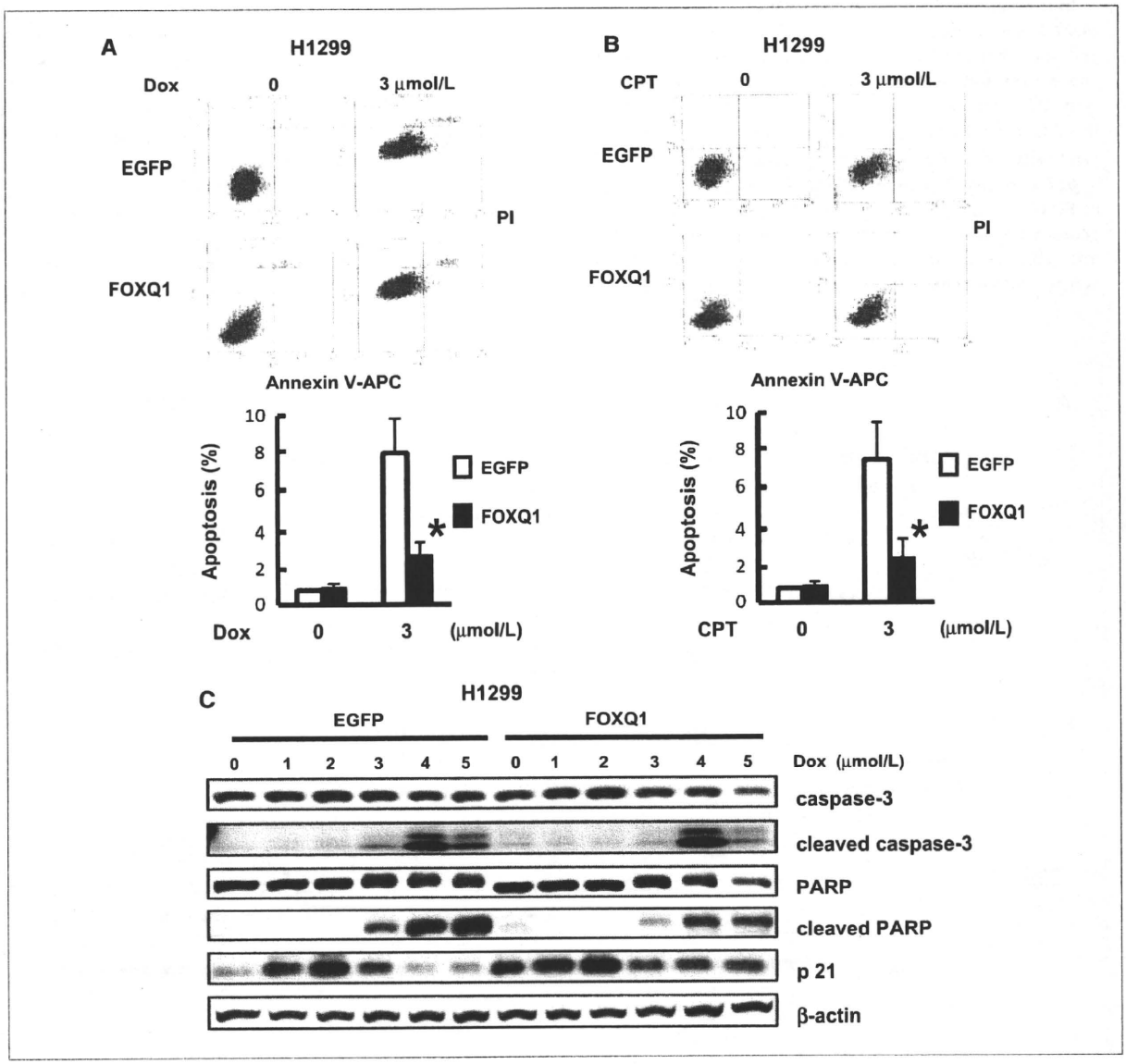

Figure 4. Overexpression of FOXQ1 promotes an antiapoptotic effect. Stable H1299 cell lines expressing EGFP or FOXQ1 (H1299/EGFP, H1299/FOXQ1) were exposed to doxorubicin (A) or camptothecin (B) at a final concentration of 3 μmol/L. Apoptotic cells were detected by Annexin V and propidium iodide (PI) using flow cytometry. C, Western blot analysis for apoptosis-related molecules. EGFP- or FOXQ1-expressing cells were exposed to doxorubicin at the indicated doses (0–5 μmol/L) for 24 h. β-Actin was used as an internal control. Dox, doxorubicin; CPT, camptothecin; EGFP, H1299/EGFP; FOXQ1, H1299/FOXQ1. *, $P < 0.05$.

Western blot analysis in DLD-1 cells. The results indicated that both sequences of FOXQ1-siRNA (FQ#1 and FQ#4) downregulated p21 expression at both the mRNA and protein levels. In addition, we confirmed the downregulation of p21 by FOXQ1-siRNA in other cell lines (WiDr and HEK293), obtaining similar results (Supplementary Fig. S1).

FOXQ1 directly increases the transcription activity of p21. We performed a luciferase reporter assay to determine whether FOXQ1 regulates p21 expression at the transcriptional level. A 2.4-kb section of the p21 promoter region was subcloned into a luciferase vector according to a previously described method (13, 28). The p21 promoter activity was increased by >8-fold when cotransfected with a FOXQ1 expression vector, compared with an empty vector (Fig. 2C). To determine whether FOXQ1 directly binds to p21 promoter, we transfected Myc or Myc-tagged FOXQ1 vectors into HEK293 cells and then conducted ChIP experiments. A segment of the *p21* promoter containing putative FOXQ1 binding site (−2264 to −1971) is precipitated with specific antibody, only if, FOXQ1 was induced (Fig. 2D).

The result indicates that FOXQ1 binds to the *p21* promoter and upregulates p21 transcriptional activity.

p53-independent p21 induction by FOXQ1 in cancer cells. Because p53 is the most important regulatory molecule of p21, we examined the downregulation of p21 by FOXQ1-siRNA in several cell lines with p53–wild type, p53-mutant, or p53-null statuses. These cell lines were transfected with control-siRNA or FOXQ1-siRNA, and p21 induction was enhanced by doxorubicin (29–31). The experiments were performed using three p53–wild type cell lines, three p53-mutation cell lines, and one p53-null cell line (Fig. 3A–C). Without doxorubicin exposure, all seven cell lines showed that p21 expression was downregulated by FOXQ1-siRNA. Notably, with doxorubicin exposure, considerable p21 downregulation by FOXQ1-siRNA was observed in the p53-mutation and p53-null cell lines, compared with in the p53–wild type cell lines. In the p53-null H1299 cell line, FOXQ1-siRNA completely suppressed p21 expression. These results suggest that p21 induction by FOXQ1 is p53 independent. An immunofluorescence study of p21 in H1299 cells also showed that p21 was completely downregulated by FOXQ1-siRNA (Fig. 3D).

Overexpression of FOXQ1 increases p21 expression and exhibits an antiapoptotic effect in cancer cells. Next, we established a stable *FOXQ1*-overexpressing cell line to confirm the induction of p21 expression by FOXQ1 and to detect any changes in the cellular phenotype of the cancer cells. FOXQ1 overexpression induced p21 expression (both mRNA and protein) in HEK293 and CoLo320 cells (Supplementary Fig. S1). Notably, p21 protein expression was markedly induced by >10-fold in the H1299/FOXQ1 cells (Supplementary Fig. S1). These results indicated that FOXQ1 robustly induces p21 expression, consistent with the findings of the siRNA study.

p21 induces an antiapoptotic effect and exerts a protective role against apoptosis induced by DNA damage. To

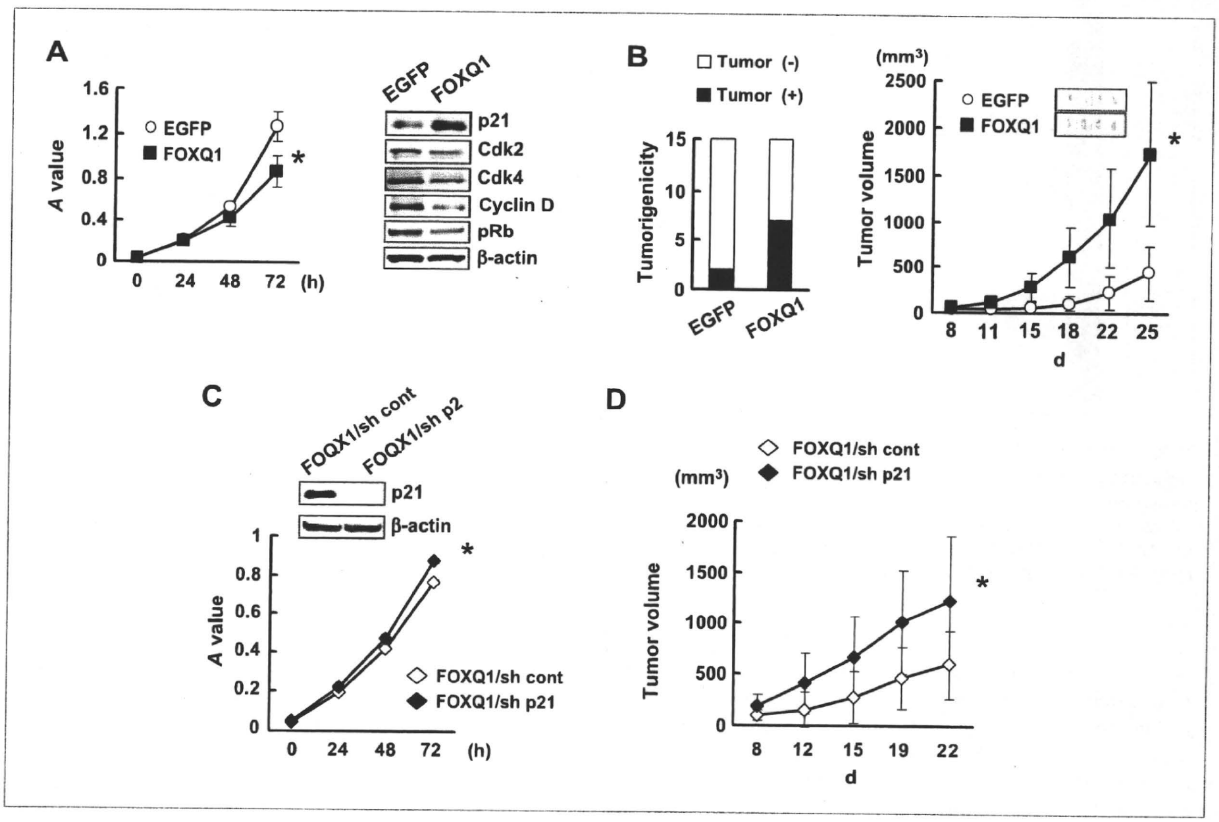

Figure 5. Overexpression of FOXQ1 enhances tumorigenicity and tumor growth *in vivo*. A, cellular growth and immunoblotting analysis of H1299 cell lines stably expressing EGFP or FOXQ1 (H1299/EGFP, H1299/FOXQ1). A total of 2×10^3 cells of each cell line were seeded in 96-well plates and evaluated after 0, 24, 48, and 72 h using MTT assay. Error bars, SD. Protein levels of H1299/EGFP and H1299/FOXQ1 cells were examined by Western blotting using specific antibody to p21, Cdk2, Cdk4, cyclin D, and phosphorylated Rb (pRb) protein. β-Actin was used as an internal control. EGFP, stable EGFP-overexpressing cells; FOXQ1, stable FOXQ1-overexpressing cells. B, H1299/EGFP and H1299/FOXQ1 cells were evaluated for their tumorigenicity *in vivo*. Mice ($n = 15$) were s.c. inoculated with a total of 1×10^6 cells. The numerical data indicate the number of mice. A total of 6×10^6 H1299/EGFP or H1299/FOXQ1 cells were s.c. inoculated into the right flank of each mouse to evaluate the tumor growth *in vivo* ($n = 12$). Representative H&E staining of tumor specimens was also shown. C, stable p21 knockdown or control cells obtained from H1299/FOXQ1 cells (H1299/FOXQ1/sh-control and H1299/FOXQ1/sh-p21) were evaluated for cellular growth and immunoblotting analysis. D, a total of 6×10^6 H1299/FOXQ1/sh-control or H1299/FOXQ1/sh-p21 cells were s.c. inoculated into the right flank of each mouse to evaluate the tumor growth ($n = 10$). *, $P < 0.05$.

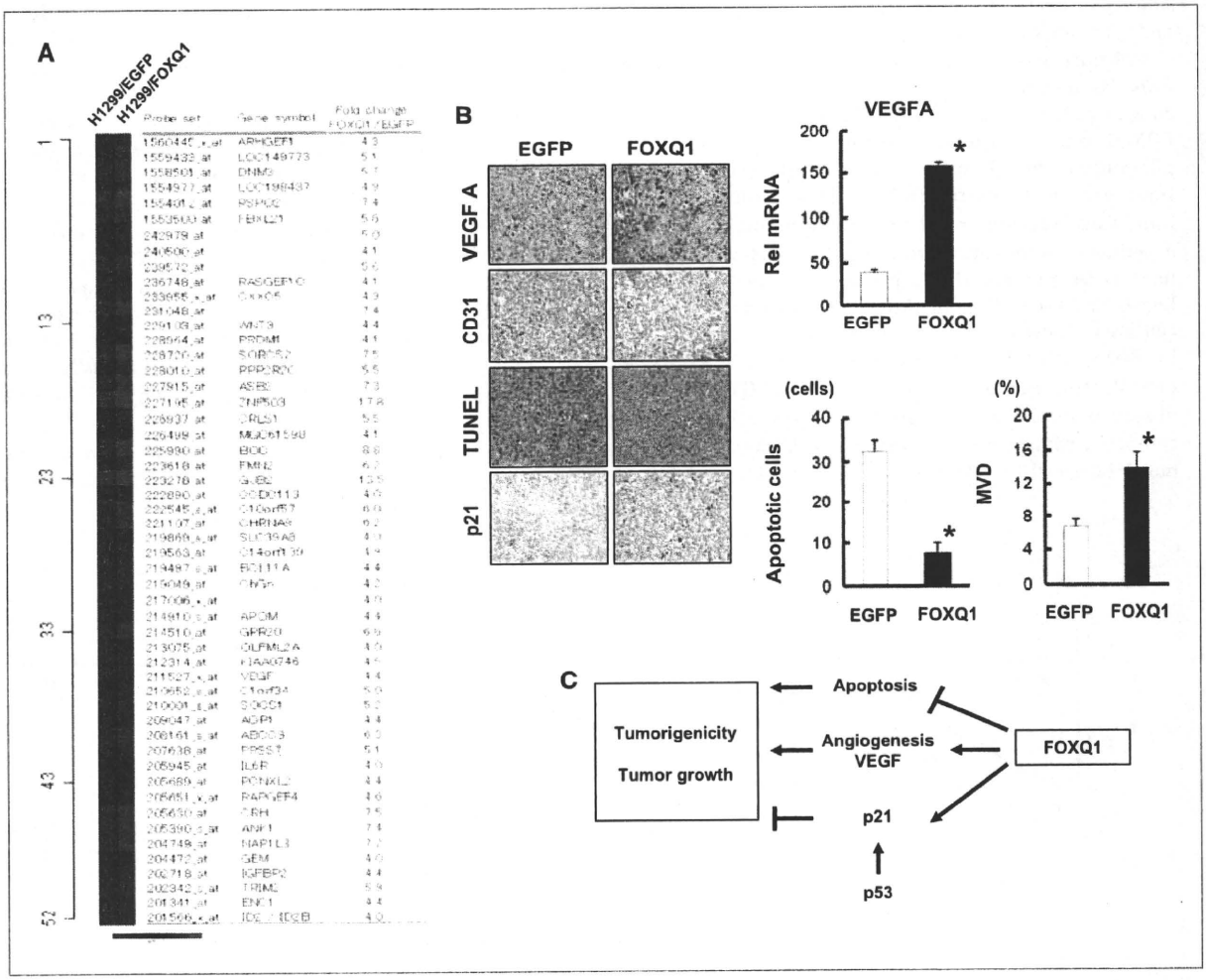

Figure 6. FOXQ1 promotes angiogenic and antiapoptotic effects *in vivo*. A, microarray analysis for H1299/EGFP or H1299/FOXQ1 cells. The upregulated genes over 4-fold by FOXQ1 were shown in the list. B, the mRNA expression levels of *VEGFA* were determined using a real-time RT-PCR analysis. Rel mRNA, normalized mRNA expression levels (*VEGFA/GAPD* × 10^4). VEGF, CD31, TUNEL, and p21 staining of tumor specimens inoculated with H1299/EGFP or H1299/FOXQ1 cells. Microvessel density (MVD) was determined by CD31-positive endothelial cells in tumor specimens using computer-assisted image analysis (Image J software package). C, diagram of a proposed mechanism of FOXQ1 for tumorigenicity and tumor growth. *, $P < 0.05$.

elucidate the role of apoptosis induced by FOXQ1 in cancer cells, we examined the apoptotic effect in H1299/EGFP and H1299/FOXQ1 cells using anticancer drugs. The overexpression of FOXQ1 inhibited the apoptosis induced by doxorubicin (H1299/EGFP: 7.9 ± 1.9%, H1299/FOXQ1: 2.7 ± 0.7%; Fig. 4A). Similarly, camptothecin-induced apoptosis was also inhibited in FOXQ1-overexpressing cells (H1299/EGFP: 7.4 ± 2.1%, H1299/FOXQ1: 2.5 ± 1.0%; Fig. 4B). Western blotting revealed that FOXQ1 overexpression decreased the levels of cleaved caspase-3 and cleaved PARP induced by doxorubicin (Fig. 4C). These results are consistent with those obtained using flow cytometry.

***Overexpression of FOXQ1 decreases cellular proliferation but enhances tumorigenicity and tumor growth* in vivo.** Stable H1299/FOXQ1 cells showed decreased cellular proliferation compared with control cells *in vitro* (Fig. 5A). Expressions of Cdk4, cyclin D1, and Cdk2 were decreased by FOXQ1 expression in H1299/FOXQ1 cells and resulted in a decrease of phosphorylated Rb expression (Fig. 5A). To examine the biological functions of FOXQ1 overexpression *in vivo*, we evaluated tumorigenicity and tumor growth using H1299/EGFP or H1299/FOXQ1 cells. H1299/FOXQ1 cells exhibited a significantly elevated level of tumorigenesis *in vivo* (GFP 2/15, FOXQ1 7/15, $P < 0.05$; Fig. 5B). In addition, the tumor volume was markedly larger in H1299/FOXQ1 cells than in H1299/EGFP cells (EGFP: 437 ± 301, FOXQ1: 1735 ± 769 mm^3, $P < 0.001$; Fig. 5B) on day 25.

***p21 does not contribute to FOXQ1-mediated tumor growth* in vivo.** Because emerging evidence has indicated that p21 may have dual functions with regard to tumor

progression and the suppression of cancer cells (32, 33), the shRNA targeting p21 or shRNA control viral vectors were further introduced into the H1299/FOXQ1 cells to elucidate the involvement of p21 in increased FOXQ1-mediated tumorigenicity and tumor growth *in vivo*. Stable H1299/FOXQ1/sh-p21 cells were slightly increased in cellular proliferation *in vitro* (Fig. 5C). In addition, tumor growth of H1299/FOXQ1/sh-p21 cells was increased compared with control cells *in vivo* (Fig. 5D). The results clearly indicate that p21 has negative roles for cellular proliferation and tumor growth in FOXQ1-overexpressing cells, suggesting that p21 does not contribute to FOXQ1-mediated tumor growth in FOXQ1-overexpressing cells *in vivo*.

***Overexpression of FOXQ1 promotes angiogenesis and antiapoptosis* in vivo.** To gain an insight into the mechanism by which FOXQ1 enhances tumor growth *in vivo*, we performed the microarray analysis on H1299/EGFP and H1299/FOXQ1 cells. Fifty-two genes were upregulated over 4-fold by overexpression of FOXQ1 including several genes that have positive roles for tumor growth, such as *VEGFA, WNT3A, RSPO2*, and *BCL11A* (Fig. 6A). Overexpression of FOXQ1 upregulated the *VEGFA* expression for 4.4-fold, suggesting the possibility of enhanced angiogenesis. Real-time RT-PCR for these cells and vascular endothelial growth factor (VEGF) staining of tumor specimens confirmed the result (Fig. 6B). Furthermore, CD31 staining of the tumor specimens showed that FOXQ1 overexpression significantly increased the angiogenesis *in vivo*.

Terminal deoxynucleotidyl transferase-mediated dUTP nick end labeling (TUNEL) and p21 immunostaining of the tumor specimens showed that p21 expression was increased and apoptosis was inhibited in H1299/FOXQ1 cells (Fig. 6B). These results strongly suggest that FOXQ1 promotes tumorigenicity and tumor growth with its angiogenic and antiapoptotic properties *in vivo* (Fig. 6C).

Discussion

FOX transcription factors are an evolutionarily conserved superfamily that control a wide spectrum of biological processes. Several Fox gene family members are involved in the etiology of cancer. Only the FOXO family has been regarded as *bona fide* tumor suppressors that promote apoptosis and cell cycle arrest at G_1 (34, 35). The loss of FOXO function observed in alveolar rhabdomyosarcoma through chromosomal translocation was first identified in relation to cancer. Many target genes of FOXO have been reported to date, including p21, cyclin D, Bim, TRAIL, and ER-α (36). On the other hand, the overexpression of FOXM is observed in head and neck cancer, breast cancer, and cervical cancer, and it enhances proliferation and tumor growth *in vitro* (37), suggesting that *FOXM* may be an oncogene. Although the available evidence is not conclusive, FOXP, FOXC, and FOXA have been linked to tumorigenesis and progression of certain cancers (36). Thus, the FOX family is thought to act as either an oncogene or a tumor suppressor. In the present study, we showed that the overexpression of FOXQ1 played a tumor-promoting role in CRC.

The p21 promoter region contains several definitive DNA regulatory elements, such as the p53-binding domain, E-box, Smad binding element, and TGF-β response elements. In the case of the other FOX family member FOXO, a recent report showed that the p21 promoter contains a consensus forkhead binding element (GGATCC) immediately upstream of the first Smad binding element and that the FOXO and Smad complexes activate p21 expression, whereas the FOXG1 protein binds to FOXO and blocks p21 induction (38). On the other hand, the consensus binding sequence (5′-NA(A/T)TGTTTA(G/T)(A/T)T-3′) has been defined for human FOXQ1 (4). The p21 promoter region contains several putative FOXQ1 binding sites according to its consensus binding sequence. Indeed, we have shown that FOXQ1 binds to a segment of the p21 promoter, indicating that FOXQ1 directly transactivates the p21 gene expression.

The initial descriptions of p21 were thought to indicate a tumor suppressor–like role, and p21 was almost solely regarded as a modulator with the principal function of inhibiting a cyclin-dependent kinase activity and, hence, cell cycle progression, because it was originally identified as a mediator of p53-induced growth arrest. However, emerging evidence has indicated that p21 may have dual functions with regard to tumor progression and the suppression of cancer cells, with examples of other genes with dual functions including TGF-β, Notch, Runx3, E2F, and p21 (32). Besides its growth inhibitory role, p21 is known to have a positive effect on cell proliferation (39–41). A more recent study on leukemic stem cells showed a p21-dependent cellular response that leads to reversible cell cycle arrest and DNA repair; such data clearly illustrate the oncogenic potential of p21 (33). We have shown that p21 has negative roles for tumor growth using FOXQ1-overexpressing cells with knockdown of p21 (Fig. 5D).

Recently, accumulating evidence has shown that FOX transcriptional factors are involved in VEGF regulation and angiogenesis. For example, forkhead has exhibited a positive role in mediating induction of VEGF (42–44). In the present study, we identified *VEGFA* as a candidate target gene of FOXQ1 by microarray analysis and showed that FOXQ1 increased angiogenesis *in vivo*. Interestingly, although overexpression of FOXQ1 decreases cellular proliferation *in vitro*, it enhances tumorigenicity and tumor growth *in vivo*. We consider that this discrepancy can be explained by these angiogenic and antiapoptotic effects of FOXQ1 contribute to enhanced tumor growth *in vivo*, although p21 negatively functions.

We showed that the overexpression of FOXQ1 inhibited doxorubicin-induced and camptothecin-induced apoptosis in p53-inactivated cancer cells. Therefore, we speculated that FOXQ1 might be a new determinant factor of resistance to drug-induced apoptosis and might represent a poor prognostic factor for CRC patients.

In conclusion, FOXQ1 is markedly overexpressed in CRC and enhances tumorigenicity and tumor growth *in vivo*. We have elucidated a biological function of FOXQ1, which directly upregulates p21 transcription and promotes angiogenesis and antiapoptosis. Our findings support FOXQ1

as a new member of the cancer-related FOX family in cancer cells.

Disclosure of Potential Conflicts of Interest

No potential conflicts of interest were disclosed.

Acknowledgments

We thank Dr. Richard Simon and Dr. Amy Peng for providing us with the BRB ArrayTools software. This free software was very useful and has been developed for user-friendly applications. We also thank Eiko Honda and Shinji Kurashimo for technical assistance.

Grant Support

Third-Term Comprehensive 2nd term of the 10-Year Strategy for Cancer Control, the program for the promotion of Fundamental Studies in Health Sciences of the National Institute of Biomedical Innovation, Scientific Research from the Ministry of Education, Culture, Sports, Science and Technology of Japan grant-in-aid, and Research Resident Fellowship from the Foundation of Promotion of Cancer Research in Japan (H. Kaneda).

The costs of publication of this article were defrayed in part by the payment of page charges. This article must therefore be hereby marked *advertisement* in accordance with 18 U.S.C. Section 1734 solely to indicate this fact.

Received 06/18/2009; revised 10/28/2009; accepted 12/01/2009; published OnlineFirst 02/09/2010.

References

1. Jonsson H, Peng SL. Forkhead transcription factors in immunology. Cell Mol Life Sci 2005;62:397–409.
2. Carlsson P, Mahlapuu M. Forkhead transcription factors: key players in development and metabolism. Dev Biol 2002;250:1–23.
3. Tran H, Brunet A, Griffith EC, Greenberg ME. The many forks in FOXO's road. Sci STKE 2003;2003:RE5.
4. Overdier DG, Porcella A, Costa RH. The DNA-binding specificity of the hepatocyte nuclear factor 3/forkhead domain is influenced by amino-acid residues adjacent to the recognition helix. Mol Cell Biol 1994;14:2755–66.
5. Hoggatt AM, Kriegel AM, Smith AF, Herring BP. Hepatocyte nuclear factor-3 homologue 1 (HFH-1) represses transcription of smooth muscle-specific genes. J Biol Chem 2000;275:31162–70.
6. Martinez-Ceballos E, Chambon P, Gudas LJ. Differences in gene expression between wild type and Hoxa1 knockout embryonic stem cells after retinoic acid treatment or leukemia inhibitory factor (LIF) removal. J Biol Chem 2005;280:16484–98.
7. Hong HK, Noveroske JK, Headon DJ, et al. The winged helix/forkhead transcription factor Foxq1 regulates differentiation of hair in satin mice. Genesis 2001;29:163–71.
8. Potter CS, Peterson RL, Barth JL, et al. Evidence that the satin hair mutant gene Foxq1 is among multiple and functionally diverse regulatory targets for Hoxc13 during hair follicle differentiation. J Biol Chem 2006;281:29245–55.
9. Goering W, Adham IM, Pasche B, et al. Impairment of gastric acid secretion and increase of embryonic lethality in Foxq1-deficient mice. Cytogenet Genome Res 2008;121:88–95.
10. Verzi MP, Khan AH, Ito S, Shivdasani RA. Transcription factor foxq1 controls mucin gene expression and granule content in mouse stomach surface mucous cells. Gastroenterology 2008; 135:591–600.
11. Harper JW, Adami GR, Wei N, Keyomarsi K, Elledge SJ. The p21 Cdk-interacting protein Cip1 is a potent inhibitor of G_1 cyclin-dependent kinases. Cell 1993;75:805–16.
12. Xiong Y, Hannon GJ, Zhang H, Casso D, Kobayashi R, Beach D. p21 is a universal inhibitor of cyclin kinases. Nature 1993;366:701–4.
13. el-Deiry WS, Tokino T, Velculescu VE, et al. WAF1, a potential mediator of p53 tumor suppression. Cell 1993;75:817–25.
14. Brugarolas J, Moberg K, Boyd SD, Taya Y, Jacks T, Lees JA. Inhibition of cyclin-dependent kinase 2 by p21 is necessary for retinoblastoma protein-mediated G_1 arrest after γ-irradiation. Proc Natl Acad Sci U S A 1999;96:1002–7.
15. Sherr CJ, Roberts JM. CDK inhibitors: positive and negative regulators of G_1-phase progression. Genes Dev 1999;13:1501–12.
16. Garner E, Raj K. Protective mechanisms of p53-21-pRb proteins against DNA damage-induced cell death. Cell Cycle 2008;7:277–82.
17. Maki CG, Howley PM. Ubiquitination of p53 and p21 is differentially affected by ionizing and UV radiation. Mol Cell Biol 1997;17:355–63.
18. Gartel AL, Tyner AL. Transcriptional regulation of the p21((WAF1/CIP1)) gene. Exp Cell Res 1999;246:280–9.
19. Gartel AL, Tyner AL. The role of the cyclin-dependent kinase inhibitor p21 in apoptosis. Mol Cancer Ther 2002;1:639–49.
20. Yamanaka R, Arao T, Yajima N, et al. Identification of expressed genes characterizing long-term survival in malignant glioma patients. Oncogene 2006;25:5994–6002.
21. Tanaka K, Arao T, Maegawa M, et al. SRPX2 is overexpressed in gastric cancer and promotes cellular migration and adhesion. Int J Cancer 2009;124:1072–80.
22. Takeda M, Arao T, Yokote H, et al. AZD2171 shows potent antitumor activity against gastric cancer over-expressing fibroblast growth factor receptor 2/keratinocyte growth factor receptor. Clin Cancer Res 2007;13:3051–7.
23. United Kingdom Co-ordinating Committee on Cancer Research (UKCCCR). Guidelines for the Welfare of Animals in Experimental Neoplasia (Second Edition). Br J Cancer 1998;77:1–10.
24. Iwasa T, Okamoto I, Suzuki M, et al. Inhibition of insulin-like growth factor 1 receptor by CP-751,871 radiosensitizes non-small cell lung cancer cells. Clin Cancer Res 2009;15:5117–25.
25. Shimada K, Nakamura M, Anai S, et al. A novel human AlkB homologue, ALKBH8, contributes to human bladder cancer progression. Cancer Res 2009;69:3157–64.
26. Igarashi T, Izumi H, Uchiumi T, et al. Clock and ATF4 transcription system regulates drug resistance in human cancer cell lines. Oncogene 2007;26:4749–60.
27. Bieller A, Pasche B, Frank S, et al. Isolation and characterization of the human forkhead gene FOXQ1. DNA Cell Biol 2001;20:555–61.
28. Datto MB, Yu Y, Wang XF. Functional analysis of the transforming growth factor β responsive elements in the WAF1/Cip1/p21 promoter. J Biol Chem 1995;270:28623–8.
29. Mahyar-Roemer M, Roemer K. p21 Waf1/Cip1 can protect human colon carcinoma cells against p53-dependent and p53-independent apoptosis induced by natural chemopreventive and therapeutic agents. Oncogene 2001;20:3387–98.
30. Mukherjee S, Conrad SE. c-Myc suppresses p21WAF1/CIP1 expression during estrogen signaling and antiestrogen resistance in human breast cancer cells. J Biol Chem 2005;280:17617–25.
31. Seoane J, Le HV, Massague J. Myc suppression of the p21(Cip1) Cdk inhibitor influences the outcome of the p53 response to DNA damage. Nature 2002;419:729–34.
32. Rowland BD, Peeper DS. KLF4, p21 and context-dependent opposing forces in cancer. Nat Rev Cancer 2006;6:11–23.
33. Viale A, De Franco F, Orleth A, et al. Cell-cycle restriction limits DNA damage and maintains self-renewal of leukaemia stem cells. Nature 2009;457:51–6.
34. Brunet A, Bonni A, Zigmond MJ, et al. Akt promotes cell survival by phosphorylating and inhibiting a Forkhead transcription factor. Cell 1999;96:857–68.
35. Paik JH, Kollipara R, Chu G, et al. FoxOs are lineage-restricted redundant tumor suppressors and regulate endothelial cell homeostasis. Cell 2007;128:309–23.
36. Myatt SS, Lam EW. The emerging roles of forkhead box (Fox) proteins in cancer. Nat Rev Cancer 2007;7:847–59.
37. Kalin TV, Wang IC, Ackerson TJ, et al. Increased levels of the FoxM1 transcription factor accelerate development and progression of prostate carcinomas in both TRAMP and LADY transgenic mice. Cancer Res 2006;66:1712–20.

38. Seoane J, Le HV, Shen L, Anderson SA, Massague J. Integration of Smad and forkhead pathways in the control of neuroepithelial and glioblastoma cell proliferation. Cell 2004;117:211–23.
39. Dong Y, Chi SL, Borowsky AD, Fan Y, Weiss RH. Cytosolic p21Waf1/Cip1 increases cell cycle transit in vascular smooth muscle cells. Cell Signal 2004;16:263–9.
40. Dupont J, Karas M, LeRoith D. The cyclin-dependent kinase inhibitor p21CIP/WAF is a positive regulator of insulin-like growth factor I-induced cell proliferation in MCF-7 human breast cancer cells. J Biol Chem 2003;278:37256–64.
41. Zhang C, Kavurma MM, Lai A, Khachigian LM. Ets-1 protects vascular smooth muscle cells from undergoing apoptosis by activating p21WAF1/Cip1: ETS-1 regulates basal and inducible p21WAF1/Cip: ETS-1 regulates basal and inducible p21WAF1/Cip1 transcription via distinct *cis*-acting elements in the p21WAF/Cip1 promoter. J Biol Chem 2003;278:27903–9.
42. Banham AH, Boddy J, Launchbury R, et al. Expression of the forkhead transcription factor FOXP1 is associated both with hypoxia inducible factors (HIFs) and the androgen receptor in prostate cancer but is not directly regulated by androgens or hypoxia. Prostate 2007;67:1091–8.
43. Furuyama T, Kitayama K, Shimoda Y, et al. Abnormal angiogenesis in Foxo1 (Fkhr)-deficient mice. J Biol Chem 2004;279:34741–9.
44. Gupta S, Joshi K, Wig JD, Arora SK. Intratumoral FOXP3 expression in infiltrating breast carcinoma: its association with clinicopathologic parameters and angiogenesis. Acta Oncol 2007;46:792–7.

A Multi-Institution Phase I/II Trial of Triweekly Regimen with S-1 Plus Cisplatin in Patients with Advanced Non-small Cell Lung Cancer

Kaoru Kubota, MD, PhD,† Hiroshi Sakai, MD,‡ Nobuyuki Yamamoto, MD, PhD,§ Hideo Kunitoh, MD, PhD,†‖ Kazuhiko Nakagawa, MD, PhD,¶ Koji Takeda, MD,# Yukito Ichinose, MD,** Nagahiro Saijo, MD, PhD,*¶ Yutaka Ariyoshi, MD,†† and Masahiro Fukuoka, MD, PhD‡‡*

Introduction: To determine the dose-limiting toxicity and recommended dose (RD) of cisplatin (CDDP) combined with S-1 (tegafur, 5-chloro-2, 4-dihydroxypyridine, and potassium oxonate) for patients with non-small cell lung cancer and to evaluate efficacy and toxicity of this regimen at RD.

Methods: Patients with stages III and IV non-small cell lung cancer received 3-week cycles of treatment, each consisting of oral administration of S-1 at 80 mg/m^2 in 2 divided doses per day for 14 consecutive days, intravenous administration of CDDP (60 mg/m^2, 70 mg/m^2, or 80 mg/m^2) on the first day, and no medication during the subsequent 7 days. The primary objective of phase I study was to estimate the maximum tolerable dose and the RD, and the primary end point of phase II study was response.

Results: RD of CDDP in the analysis of 18 eligible patients was 60 mg/m^2. Evaluation of efficacy and toxicity at RD in 55 eligible patients showed that partial response was observed in 18 patients (32.7%, 95% confidence interval: 20.7–46.7%). The median survival time was 18.1 months, and the time to disease progression was 3.8 months. Grade 3 or severer adverse events were observed in 27 patients (49.1%).

Conclusions: CDDP combined with S-1 showed a satisfactory overall survival time and acceptable toxicity profile. However, the response as the primary end point did not reach the predetermined threshold level.

From the *Thoracic Oncology Division, National Cancer Center Hospital East, Kashiwa, Japan; †Division of Thoracic Oncology, National Cancer Center, Tokyo, Japan; ‡Division of Thoracic Oncology, Saitama Cancer Center, Saitama, Japan; §Division of Thoracic Oncology, Shizuoka Cancer Center, Shizuoka, Japan; ‖Division of Thoracic Oncology, Mitsui Memorial Hospital, Tokyo, Japan; ¶Department of Medical Oncology, Kinki University School of Medicine, Osaka, Japan; #Department of Clinical Oncology, Osaka City General Hospital, Osaka, Japan; **Department of Thoracic Oncology, Kyushu Cancer Center, Fukuoka, Japan; ††Prefectural Aichi Hospital, Aichi, Japan; and ‡‡Kinki University School of Medicine, Sakai Hospital, Osaka, Japan.

Disclosure: The authors declare no conflicts of interest.

Address for correspondence: Kaoru Kubota, MD, PhD, Thoracic Oncology Division, National Cancer Center Hospital, 5-1-1 Tsukiji, Chuo-ku, Tokyo 104-0045, Japan. E-mail: kkubota@ncc.go.jp

ISSN: 1556-0864/10/0505-0702

Key Words: S-1, NSCLC (non-small cell lung cancer), Chemotherapy, Phase I/II trial, Cisplatin.

(*J Thorac Oncol.* 2010;5: 702–706)

Lung cancer, with its high mortality rate, is the most common cause of death from malignant tumors. Among the various types of lung cancer, non-small cell lung cancer (NSCLC) accounts for more than 80% of all patients with lung cancer. Platinum-based two-drug combinations with third-generation agents such as docetaxel,[1] paclitaxel,[2] gemcitabine,[3] and vinorelbine[4] are standard first-line treatment for metastatic NSCLC. Cisplatin (CDDP) plus pemetrexed or carboplatin, paclitaxel plus bevacizumab is an option for nonsquamous NSCLC.[5,6] Platinum-based chemotherapy has also been applied to combined modality treatment with thoracic radiotherapy or surgery in stage II, IIIA, or IIIB NSCLC.[7–9] Although chemotherapy plays an important role in the management of patients with NSCLC, the benefits of chemotherapy are modest and standard platinum-based regimens have significant toxicities; thus, more effective and less toxic regimens are needed. Although an important goal of such development is to raise the survival rate, it is also crucial to minimize adverse events, cost, and improve quality of life.

S-1 (Taiho Pharmaceutical Co., Ltd., Tokyo, Japan) is an oral antineoplastic drug consisting of tegafur, which is a prodrug of 5-fluorouracil (5-FU), and 2 modulators, 5-chloro-2,4-dihydroxypyridine and potassium oxonate.[10] Tegafur has advantages of high bioavailability and small individual differences in absorption. This substance is gradually converted to 5-FU in liver. On the other hand, 5-chloro-2,4-dihydroxypyridine antagonizes dihydropyrimidine dehydrogenase and suppresses the metabolism of 5-FU in liver to help maintain the blood level of 5-FU[11] and prevents neurotoxicity by suppressing the generation of metabolite F-β-alanine. Potassium oxonate prevents gastrointestinal toxicity through inhibition of orotate phosphoribosyl transferase and suppresses the phosphorylation of 5-FU in the digestive tract.[12–14]

Ichinose et al.[15] conducted a phase II study on the combination of S-1 and CDDP chemotherapy in patients with

advanced NSCLC, using the schedule defined by a phase I study in patients with advanced gastric cancer (3-week administration of S-1 with CDDP at 60 mg/m^2 on day 8). Because the approved dose of CDDP for NSCLC in Japan is 70 to 90 mg/m^2 and many regimens use day 1 administration of CDDP in a 3-week schedule, the Health, Labor and Welfare Ministry of Japan requested to evaluate the day 1 administration of CDDP and S-1 in a 3-week schedule. For this reason, we conducted the phase I/II study with 2-week administration of S-1 combined with CDDP on day 1.

The purpose of the study is to define maximum tolerated dose (MTD) and recommended dose (RD) of CDDP in the phase I study and evaluated response rate, survival, and adverse events in the phase II study.

PATIENTS AND METHODS

Patient Eligibility

Patients satisfying the following criteria were eligible: (1) clinical stage of IIIB (no indications of radical radiotherapy) or IV with a diagnosis of NSCLC confirmed by histology or cytology; (2) presence of a measurable lesion; (3) age 20 to 74 years at the time of enrollment; (4) Eastern Cooperative Oncology Group performance status of 0 to 1; and (5) expected survival time of 3 months or more. Other eligibility criteria included white blood cells (4 to 12 $\times$ 10^3/μl), platelets ($\geq$100 $\times$ 10^3/μl), hemoglobin ($\geq$9.0 g/dl), total bilirubin ($\leq$1.5 times laboratory reference value), aspartate aminotransferase and alanine aminotransferase ($\leq$100 U/liter), alkaline phosphatase ($\leq$2 times normal laboratory reference value), creatinine clearance ($\geq$60 ml/min), and oxygen partial pressure ($\geq$60 mmHg). Exclusion criteria included (1) patients with a history of severe drug sensitivity (not specified); (2) patients taking other anticancer medication; (3) patients with active infection; (4) patients with significant comorbid medical conditions, including, but not limited to, heart failure, renal failure, hepatic failure, hemorrhagic peptic ulcer, mechanical or paralytic ileus, or poorly controlled diabetes; (5) patients with pleural effusion, ascites, or pericardial fluid requiring drainage; (6) patients with symptomatic brain metastasis; (7) patients with difficulty in controlling bowel movements; (8) patients with prior malignancies within the past 5 years of nontreatment or disease-free interval, with the exception of carcinoma in situ; (9) pregnant, nursing, or potentially pregnant women; and (10) patients considered inappropriate by the principal or subinvestigator. The patients meeting enrollment criteria were registered after obtaining their written informed consent. This protocol was reviewed and approved by institutional review boards at all participating institutes.

Treatment Schedule

CDDP was administered on the first day with 14 consecutive day administration of S-1 and no medication on the subsequent 7 days (21 days in total). S-1 was prescribed at a dose of 80 mg/d if body surface area was less than 1.25 m^2, 100 mg/d if body surface area was 1.25–1.5 m^2, or 120 mg/d if body surface area was 1.5 m^2 or more, divided into 2 doses/d. The dose of S-1 was reduced by one level (20 mg/d) in patients with BSA $\geqq$1.25 m^2 if there were grade 4 leukocytopenia, neutropenia, or platelet counts below 10,000/mm^3 or grade 3 or more nonhematological toxicity including diarrhea, stomatitis, or rash. If the dose reduction was required in patients who received 80 mg/d (patients with BSA $<$1.25 m^2 or who had dose reduction) it was reduced to a minimum of 50 mg/d.

Analysis for MTD and RD of CDDP (Phase I Trial)

RD Analysis

Doses of CDDP in the estimation of MTD were set in increments of 10 mg/m^2 starting from a dose of 70 mg/m^2 (level 1). RD was defined as the dose that was one level lower than MTD. If MTD was defined as more than 80 mg/m^2 (level 2), no further dose increase was made, and RD was set at 80 mg/m^2.

MTD Analysis

MTD was estimated based on the analysis of dose-limiting toxicity (DLT) as follows: (1) If DLT occurrence was 0/3, CDDP dose was increased to 80 mg/m^2; (2) If DLT occurrence ranged from 1/3 to 2/3, 3 patients were added, and 70 mg/m^2 of CDDP was repeated; (3) If DLT occurrence was 3/3, this level was judged as MTD; (4) If DLT occurrence after adding 3 patients ranged from 1/6 to 2/6, CDDP dose was increased to 80 mg/m^2; and (5) If DLT occurrence was 3/6 or more, this level was judged as MTD. The same procedures were repeated at the CDDP dose of 80 mg/m^2, except the dose was not increased further. If MTD was not determined at 80 mg/m^2, it was estimated to be more than 80 mg/m^2. The level was evaluated at least 1 week after the completion of protocol treatment.

Definition of DLT

DLT was defined by the following adverse events: (1) persistence of grade 4 neutropenia for 4 days or more; (2) neutropenic fever of 38°C or more; (3) grade 3 or 4 for thrombocytopenia; (4) grade 3 or more severe nonhematologic toxicity other than nausea, vomiting, anorexia, and hyponatremia; and (5) any adverse event requiring reduction of total S-1 dose below 75% of the planned dose per cycle.

Assessment of Response

Antitumor response was evaluated by computed tomography scan and magnetic resonance imaging at 4-week intervals after the beginning of administration in comparison with the baseline lesions taken within 2 weeks before enrollment using "Response Evaluation Criteria in Solid Tumors (RECIST) Guidelines."

Safety Assessment

Adverse events were identified according to "National Cancer Institute Common Toxicity Criteria (NCI-CTC), Version 2.0."

Sample Size Determination and Statistical Analysis

Assuming the response would follow a binomial distribution, enrollment of 54 patients was planned, so that an expected response of 50% would be significant in a test at the one-tailed significance level of $\alpha/2$ = 2.5% when the thresh-

old response is 30% and the power of the test ($1 - \beta$) is 80%. The survival curve for eligible patients was estimated using Kaplan-Meier method,[16] and median survival time (MST), 1-year, and 2-year survival proportions were calculated.

RESULTS

Eligible Patients and Doses

From seven institutions in Japan, 18 patients were enrolled in the phase I and 55 eligible patients in the phase II study. The latter included six patients accrued in phase I at RD. Table 1 shows characteristics of the total 67 patients. Patients were enrolled between July 2004 and August 2005.

Recommended Dose

MTD and RD of CDDP were estimated with six patients in the 70 mg/m^2 dose group (level 1) and six patients in the 80 mg/m^2 dose group (level 2), respectively. Severe adverse events that should be regarded as DLT, such as shock, disseminated intravascular coagulation, and bloody stool, occurred in three patients (50.0%, three of six) during second and later cycles in level 1. Thus, we considered that level 1 corresponded to MTD and performed an additional evaluation at the CDDP dose of 60 mg/m^2 assigned as level 0 in six patients. In the 60 mg/m^2 group (level 0), one patient developed pneumonia during the second cycle, but no other events corresponding to DLT were observed. Therefore, we estimated that MTD of CDDP in this schedule was 70 mg/m^2 and RD was level 0.

Compliance

We regarded as completion of a cycle if CDDP was administered on the first day, and the patient took 28 doses of S-1. The number of patients completing 1, 2, 3, and 4 or more cycles was 50, 36, 34, and 25, respectively. The reasons of noncompletion were adverse events in 11 patients, disease progression in 6 patients, and refusal and inadvertent skipping in 3 patients. In this trial, it was possible to administer S-1 without dose reduction 90.9% of patients (50 of 55).

TABLE 1. Patient Characteristics

	Phase I		Phase II
CDDP (mg/m^2)	70	80	60
No. of patients	6	6	55
Gender			
Male	6	3	32
Female	0	3	23
Age, yr			
Median	57	54	59
Range	49–69	37–66	36–74
ECOG performance status			
0	2	2	20
1	4	4	35
Clinical stage			
IIIB	3	1	14
IV	3	5	41
Histology			
Adenocarcinoma	6	5	43
Squamous cell carcinoma	0	0	7
Others	0	1	5

CDDP, cisplatin; ECOG, Eastern Cooperative Oncology Group.

TABLE 2. Response by Patient Characteristics

Characteristics	No. of Patients	Response					Response (%)
		CR	PR	SD	PD	NE	
All	55	0	18	18	16	3	32.7[a]
Gender							
Male	32	0	11	10	10	1	34.4
Female	23	0	7	8	6	2	30.4
Stage							
IIIB	14	0	5	4	4	1	35.7
IV	41	0	13	14	12	2	31.7
Histology							
Adenocarcinoma	43	0	14	12	14	3	32.6
Squamous cell carcinoma	7	0	2	4	1	0	28.6
Others	5	0	2	2	1	0	40.0

CR, complete response; PR, partial response; SD, stable disease; PD, progressive disease; NE, not evaluated.
[a] 95% confidence interval: 20.7–46.7%.

Response and Survival

Table 2 shows the antitumor response (RECIST) in the 55 patients in phase II part of the study, as determined by the central review. Response was 32.7% (18 of 55), and 95% confidence interval (CI) was 20.7 to 46.7%.

In the 18 responding patients, the median time to 30% reduction in tumor size was 38 days (range, 19–60 days). The reduction occurred during the first cycle in three patients (16.7%), second cycle in seven patients (38.9%), and third cycle in eight patients (44.4%). Median time to confirmation of partial response was 75.5 days (range, 51–95 days). This occurred during the third cycle in 10 patients (55.6%), fourth cycle in 6 patients (33.3%), and fifth cycle in 2 patients (11.1%). The median response duration was 104 days (range, 57–176 days).

At the time of analysis, there were 32 cases of progression and 38 death events. MST of the 55 patients was 18.1 months (95% CI: 13.3–23.2 months), 1-year survival proportion was 65.2%, and 2-year survival proportion was 34%. The median follow-up at the time of analysis was 31.0 months (range, 29.3–33.0 months). The median time to disease progression was 3.8 months (95% CI: 3.1–5.7 months). Kaplan-Meier curves are shown in Figures 1 and 2.

Adverse Events

Major adverse events observed in this trial were myelosuppression, gastrointestinal toxicity, abnormal liver, or renal function (Table 3). No treatment-related deaths were observed in this trial.

DISCUSSION

This study was conducted to determine the optimal dose of CDDP on day1 in combination with 14-day admin-

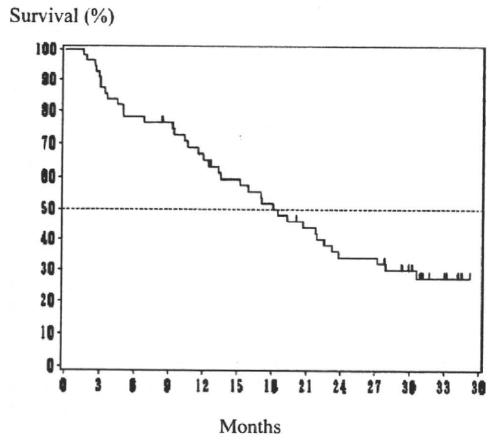

Number of patients analyzed: 55

Number of deaths: 38

Median survival time: 18.1 months (95% CI:13.3–23.2 months)

1-year survival proportion: 65.2%

2-year survival proportion: 34.0%

Time (months)	0	3	6	9	12	15	18	21	24	27	30	33
At risk	55	50	43	41	36	31	27	22	17	17	12	5

FIGURE 1. Overall survival.

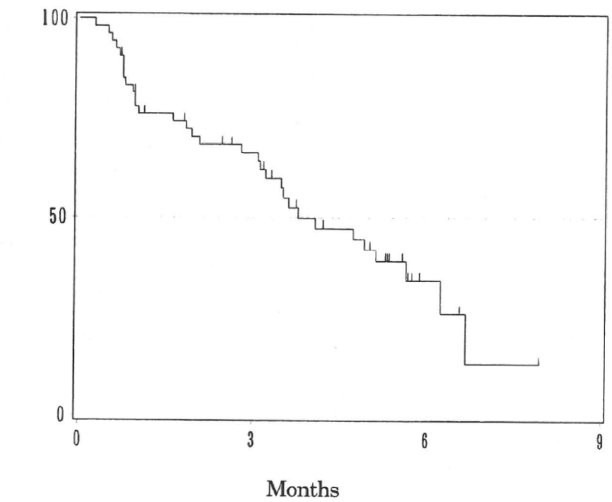

Number of patients analyzed: 55

Number of deaths: 32

Median survival time: 3.8months (95% CI:3.1–5.7 months)

Time (months)	0	1	2	3	4	5	6	7	8
At risk	55	44	35	31	20	16	4	1	1

FIGURE 2. Time to progression.

TABLE 3. Hematologic and Nonhematologic Toxicities (All Cycles)[a]

	Phase I					Phase II (Including 60 mg/m² in Phase I)									
CDDP (mg/m²)	70					80					60				
No. of Patients	6					6					55				
	Grade					Grade					Grade				
Toxicity	**1**	**2**	**3**	**4**	**≧3**	**1**	**2**	**3**	**4**	**≧3**	**1**	**2**	**3**	**4**	**≧3**
Leukopenia	1	1	2	1	3	1	1	2	—	2	16	11	3	—	3
Neutropenia	1	1	1	2	3	1	2	—	1	1	12	9	9	3	12
Anemia	3	1	1	1	2	3	—	2	—	2	20	18	5	2	7
Thrombocytopenia	3	1	1	—	1	1	—	1	—	1	21	7	3	—	3
Aspartate aminotransferase	3	—	—	—	—	3	—	—	—	—	13	1	3	1	2
Alanine aminotransferase	2	1	—	—	—	2	—	—	—	—	17	2	1	1	2
Creatinine	2	1	—	—	—	1	—	—	—	—	14	2	1	—	1
Anorexia	1	1	2	—	2	3	1	1	—	1	28	12	10	1	11
Vomiting	1	—	—	—	—	—	3	—	—	—	16	10	3	—	3
Diarrhea	3	—	1	—	1	3	—	1	—	1	19	5	4	—	4
Stomatitis	2	—	1	—	1	—	2	—	—	—	16	6	1	—	1
Pigmentation	2	1	—	—	—	3	—	—	—	—	16	—	—	—	—
Shock	—	—	1	—	1	—	—	—	—	—	—	—	—	—	—
DIC	—	—	1	—	1	—	—	—	—	—	—	—	—	—	—
Bloody stool	—	—	—	—	—	—	—	1	—	1	—	—	—	—	—

[a] This table shows no. of patients.
DIC, disseminated intravascular coagulation.

istration of S-1 as 3-week cycle and to evaluate efficacy and safety of the regimen at RD in patients with advanced NSCLC. In phase I part of the study, MTD and RD of CDDP were defined as 70 mg/m² and 60 mg/m², respectively. RD of CDDP on day 1 was identical to day 8 administration of CDDP used in the NSCLC phase II study by Ichinose et al.,[15] which was based on RD of CDDP in combination chemotherapy for gastric cancer reported by Koizumi et al.[17]

The previous phase II study of 3-week administration of S-1 combined with 60 mg/m² of CDDP on day 8 showed objective response of 47%, MST of 11.2 months, and 1-year and 2-year survival proportions of 45% and 17%, respectively. Although we must be careful to historically compare, objective response was numerically higher in the previous study with CDDP on given day 8 than this study with CDDP on given day 1. Phase II part of this study demonstrated that response in 55 patients was 32.7% (18 of 55, 95% CI: 20.7–46.7%) and did not reach the predetermined threshold level.

Although objective response did not meet the threshold level, the results of survival were encouraging with a MST of 18.1 months, a 1-year survival proportion of 65.2%, and a 2-year survival proportion of 34%. The relatively good survival results might in part be due to second-line treatment with third-generation antineoplastic agents and/or molecular-targeted agents: 74.5% of patients received second-line chemotherapy including endothelial growth factor receptor tyrosine kinase inhibitors as poststudy treatment.

Preclinical studies showed the strongest antitumor effect was produced by the treatment with tegafur-uracil administered both before and after CDDP.[18] In addition, Satouchi et al. conducted a randomized phase II study of two different schedules of S-1 and gemcitabine in patients with advanced NSCLC. S-1 was administered daily from day 1 to 14, and gemcitabine was given on days 1 and 8 or days 8 and 15. Objective response, median time to progression, and MST were favored for gemcitabine on days 8 and 15 schedule.[19] Optimum sequence of S-1 in combination with other agents has not been determined; however, S-1 and CDDP or gemcitabine trials suggest that day 8 administration of other agents is more effective than day 1 administration in combination with S-1.

In conclusion, the RD of CDDP on day 1 was identical to that of day 8 administration of CDDP in combination with S-1 in patients with advanced NSCLC. We have chosen day 8 administration schedule of CDDP and S-1 from days 1 to 21 as experimental arm in the phase III trial currently underway.

ACKNOWLEDGMENTS

Supported by Taiho Pharmaceutical Co., Ltd., Tokyo, Japan.

The authors are indebted to Professor J. Patrick Barron of the Department of International Medical Communications of Tokyo Medical University, a remunerated consultant of Taiho Pharmaceutical Co., Ltd. for his review of this manuscript.

REFERENCES

1. Kubota K, Watanabe K, Kunitoh H, et al. Phase III randomized trial of docetaxel pluscisplatin versus vindesine plus cisplatin in patients with stage IV non-small-cell lung cancer: the Japanese Taxotere Lung Cancer Study Group. *J Clin Oncol* 2004;22:254–261.
2. Kelly K, Crowley J, Bunn PA, et al. Randomized phase III trial of paclitaxel plus carboplatin versus vinorelbine plus cisplatin in the treatment of patients with advanced non-small-cell lung cancer: a Southwest Oncology Group. *J Clin Oncol* 2001;19:3210–3218.
3. Sandler AB, Nemunaitis J, Denham C, et al. Phase III trial of gemcitabine plus cisplatin versus cisplatin alone in patients with locally advanced or metastatic non-small-cell lung cancer. *J Clin Oncol* 2000; 18:122–130.
4. Wozniak AJ, Crowley JJ, Balcerzak SP, et al. Randomized trial comparing cisplatin with cisplatin plus vinorelbine in the treatment of advanced non-small-cell lung cancer: a Southwest Oncology Group study. *J Clin Oncol* 1998;16:2459–2465.
5. Scagliotti GV, Parikh P, von Pawel J, et al. Phase III study comparing cisplatin plus gemcitabine with cisplatin plus pemetrexed in chemotherapy-naive patients with advanced-stage non-small-cell lung cancer. *J Clin Oncol* 2008;26:3543–3551.
6. Sandler A, Gray R, Perry MC, et al. Paclitaxel-carboplatin alone or with bevacizumab for non-small-cell lung cancer. *N Engl J Med* 2006;355: 2542–2550.
7. Rosell R, Gomez-Codina J, Camps C, et al. A randomized trial comparing preoperative chemotherapy plus surgery with surgery alone in patients with non-small-cell lung cancer. *N Engl J Med* 1994;330:153–158.
8. Furuse K, Fukuoka M, Kawahara M, et al. Phase III study of concurrent versus sequential thoracic radiotherapy in combination with mitomycin, vindesine, and cisplatin in unresectable stage III non-small-cell lung cancer. *J Clin Oncol* 1999;17:2692–2699.
9. Depierre A, Milleron B, Moro-Sibilot D, et al. Preoperative chemotherapy followed by surgery compared with primary surgery in resectable stage I (except T1N0), II, and IIIa non-small-cell lung cancer. *J Clin Oncol* 2002;20:247–253.
10. Shirasaka T, Shimamoto Y, Fukushima M. Inhibition by oxonic acid of gastrointestinal toxicity of 5-fluorouracil without loss of its antitumor activity in rats. *Cancer Res* 1993;53:4004–4009.
11. Tatsumi K, Fukushima M, Shirasaka T, et al. Inhibitory effects of pyrimidine, barbituric acid and pyridine derivatives on 5-fluorouracil degradation in rat liver extracts. *Jpn J Cancer Res* 1987;78:748–755.
12. Shirasaka T, Shimamato Y, Ohshimo H, et al. Development of a novel form of an oral 5-fluorouracil derivative (S-1) directed to the potentiation of the tumor selective cytotoxicity of 5-fluorouracil by two biochemical modulators. *Anticancer Drugs* 1996;7:548–557.
13. van Groeningen CJ, Peters GJ, Schornagel JH, et al. Phase I clinical and pharmacokinetic study of oral S-1 in patients with advanced solid tumors. *J Clin Oncol* 2000;18:2772–2779.
14. Yamada Y, Hamaguchi T, Goto M, et al. Plasma concentrations of 5-fluorouracil and F-beta-alanine following oral administration of S-1, a dihydropyrimidine dehydrogenase inhibitory fluoropyrimidine, as compared with protracted venous infusion of 5-fluorouracil. *Br J Cancer* 2003;89:816–820.
15. Ichinose Y, Yoshimori K, Sakai H, et al. S-1 plus cisplatin combination chemotherapy in patients with advanced non-small cell lung cancer: a multi-institutional phase II trial. *Clin Cancer Res* 2004;10:7860–7864.
16. Kaplan E, Meier P. Nonparametric estimation from incomplete observations. *J Am Stat Assoc* 1958;53:457–481.
17. Koizumi W, Tanabe S, Saigenji K, et al. Phase I/II study of S-1 combined with cisplatin in patients with advanced gastric cancer. *Br J Cancer* 2003;89:2207–2212.
18. Yamada Y, Saito H, Oie S, et al. Experimental study of the effect of combined treatment of UFT with CDDP on human solid tumor-xenografts in nude mice. *Jpn J Cancer Chemother* 1990;17:1327–1331.
19. Satouchi M, Kotani Y, Katakami N, et al. Randomized phase II study of two different schedules of gemcitabine and oral TS-1 in chemo-naive patients with advanced non-small cell lung cancer (NSCLC) (Meeting Abstracts). *J Clin Oncol* 2008;26:8103.

VOLUME 28 · NUMBER 17 · JUNE 10 2010

JOURNAL OF CLINICAL ONCOLOGY

Successful Treatment With Erlotinib After Gefitinib-Related Severe Hepatotoxicity

A 66-year-old nonsmoking woman presented with enlarged left supraclavicular lymph nodes. She had no history of liver disease, alcohol intake, or hepatitis. Baseline blood tests showed cell counts, electrolytes, as well as renal and liver function to be normal. She had not previously received medication for her condition. A chest x-ray revealed a nodular shadow in the right upper lung field. A computed tomography scan of the chest confirmed a solitary spiculated lesion in the right upper lung lobe, disseminated nodules in the interlobar fissures, and multiple pulmonary nodules. Core biopsy of left supraclavicular lymph nodes revealed adenocarcinoma, consistent with metastasis from the primary non–small-cell lung carcinoma. Mutation analysis of lung cancer specimens obtained before first-line chemotherapy showed the presence of an exon 19 deletion of the epidermal growth factor receptor gene, and gefitinib was administered orally at a dose of 250 mg once daily. Eight weeks after the initiation of treatment, computed tomography revealed marked tumor shrinkage, which was categorized as a partial response. After 13 weeks of gefitinib treatment, laboratory investigations showed a substantial increase in serum transaminase levels (AST of 84 U/L, compared with a normal range of lower than 40; ALT of 181 U/L, compared with a normal range of lower than 35; Fig 1). Initiation of treatment with ursodeoxycholic acid and ammonium glycyrrhizate resulted in a gradual decrease in transaminase levels (to values of 31 U/L and 35 U/L for AST and ALT, respectively; Fig 1). Thirty-six weeks after the initiation of daily gefitinib administration, the transaminase levels of the proband had begun to increase again, reaching a pronounced high of 599 U/L for AST and 1,011 U/L for ALT at 37 weeks (Fig 1). Gefitinib treatment was discontinued at 36 weeks. The patient had taken no other medications or supplements, and an abdominal ultrasound revealed a normal liver with no other substantial abnormalities. A drug lymphocyte stimulation test yielded a strong positive result for gefitinib, suggesting that the hepatitis of the proband was attributable to drug allergy rather than to dose-dependent toxicity. We therefore concluded that gefitinib should not be administered further at any schedule in this patient. In the 7 weeks after gefitinib withdrawal, the patient's liver function normalized but her lung cancer progressed slightly. We initiated treatment with erlotinib accompanied by careful monitoring of liver function, and the patient has continued daily oral erlotinib (150 mg) for 15 weeks with no evidence of increased hepatic toxicity or disease progression.

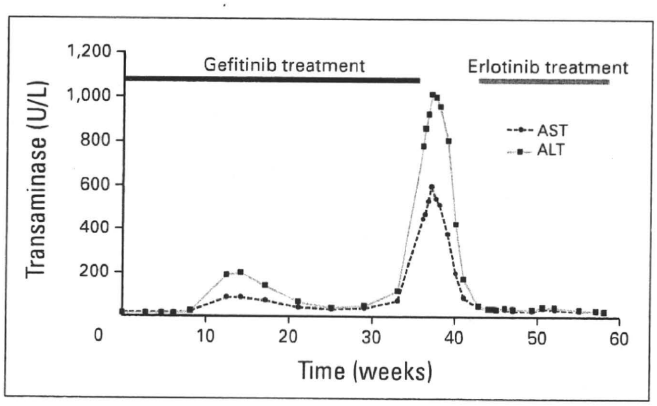

Fig 1.

Gefitinib-induced hepatitis has received little attention to date, even though phase I trials revealed hepatotoxicity as a dose-limiting toxicity of the drug and the Iressa Dose Evaluation in Advanced Lung Cancer (IDEAL 1) trial showed that 2% of patients receiving gefitinib alone at a dose of 250 mg per day developed elevations of hepatic enzymes of grade 3 or 4 that necessitated cessation of treatment.[1] Exploration of new strategies for management of gefitinib-induced severe hepatotoxicity is thus warranted. Resumption of gefitinib treatment after its discontinuation as a result of the development of drug-induced hepatitis has been reported in three cases. However, gefitinib was again discontinued because of repeated elevation of serum transaminase levels in two of three cases[2,3]; the other case showed that an intermittent schedule of gefitinib administration (250 mg/d every 5 days) reduced hepatotoxicity, although the response had been maintained for only 8 weeks at the time of report submission.[4] These findings prompted us not to recommend resumption of gefitinib treatment after the development of severe hepatotoxicity in this patient. Erlotinib acts in a manner similar to that of gefitinib and has been shown to provide clinical benefit in patients with tumors positive for epidermal growth factor receptor gene mutations. We thus treated the proband of this study with erlotinib (150 mg once daily) as an alternative to gefitinib after discontinuation of the latter drug.

With regard to the toxicity profiles of gefitinib and erlotinib, it is important to clarify the mechanism responsible for drug-induced hepatotoxicity. Gefitinib and erlotinib share a common chemical backbone structure and exhibit similar disposition characteristics in humans after oral administration. They manifest similar oral bioavailabilities and both undergo extensive metabolism primarily by cytochrome P450 3A4, with more than 80% of the administered dose being found in feces.[5,6] Administration of erlotinib at the maximum-tolerated dose and approved dose of 150 mg once daily resulted in a steady-state plasma trough concentration that was approximately 3.5 times that for gefitinib administered at the recommended dose (approximately one third of the maximum tolerated dose) of 250 mg once daily.[7,8] This patient received no medications that influence the pharmacokinetics of gefitinib or erlotinib, suggesting that the plasma concentration of gefitinib per se did not give rise to the drug-induced hepatotoxicity, although the toxicity of gefitinib has not been directly compared with that of erlotinib alone. Instead, the positive result of the drug lymphocyte stimulation test supports a diagnosis of gefitinib-induced allergic hepatitis. Erlotinib and gefitinib share a

4-anilinoquinazoline base structure, but differ in the substituents attached to the quinazoline and anilino rings. Minor differences in the chemical structures of these compounds may thus influence hepatotoxicity. In conclusion, erlotinib is an effective and well-tolerated treatment option for patients for whom gefitinib has been discontinued because of severe hepatotoxicity. Clinical trials to evaluate the administration of erlotinib after severe hepatotoxicity induced by daily administration of gefitinib are warranted.

Masayuki Takeda and Isamu Okamoto
Department of Medical Oncology, Kinki University School of Medicine, Osaka, Japan

Masahiro Fukuoka
Department of Medical Oncology, Kinki University School of Medicine, Sakai Hospital, Osaka, Japan

Kazuhiko Nakagawa
Department of Medical Oncology, Kinki University School of Medicine, Osaka, Japan

AUTHORS' DISCLOSURES OF POTENTIAL CONFLICTS OF INTEREST
The author(s) indicated no potential conflicts of interest.

REFERENCES

1. Fukuoka M, Yano S, Giaccone G, et al: Multi-institutional randomized phase II trial of gefitinib for previously treated patients with advanced non-small-cell lung cancer (The IDEAL 1 trial). J Clin Oncol 21:2237-2246, 2003
2. Ho C, Davis J, Anderson F, et al: Side effects related to cancer treatment: CASE 1. Hepatitis following treatment with gefitinib. J Clin Oncol 23:8531-8533, 2005
3. Carlini P, Papaldo P, Fabi A, et al: Liver toxicity after treatment with gefitinib and anastrozole: Drug-drug interactions through cytochrome P450? J Clin Oncol 24:e60-e61, 2006
4. Seki N, Uematsu K, Shibakuki R, et al: Promising new treatment schedule for gefitinib responders after severe hepatotoxicity with daily administration. J Clin Oncol 24:3213-3214, 2006; author reply 24:3214-3215, 2006
5. Ling J, Johnson KA, Miao Z, et al: Metabolism and excretion of erlotinib, a small molecule inhibitor of epidermal growth factor receptor tyrosine kinase, in healthy male volunteers. Drug Metab Dispos 34:420-426, 2006
6. McKillop D, McCormick AD, Millar A, et al: Cytochrome P450-dependent metabolism of gefitinib. Xenobiotica 35:39-50, 2005
7. Li J, Karlsson MO, Brahmer J, et al: CYP3A phenotyping approach to predict systemic exposure to EGFR tyrosine kinase inhibitors. J Natl Cancer Inst 98:1714-1723, 2006
8. Tan AR, Yang X, Hewitt SM, et al: Evaluation of biologic end points and pharmacokinetics in patients with metastatic breast cancer after treatment with erlotinib, an epidermal growth factor receptor tyrosine kinase inhibitor. J Clin Oncol 22:3080-3090, 2004

DOI: 10.1200/JCO.2009.26.5496; published online ahead of print at www.jco.org on April 12, 2010

Successful Treatment with Erlotinib after Gefitinib-Induced Severe Interstitial Lung Disease

Masayuki Takeda, MD, PhD, Isamu Okamoto, MD, PhD,* Chihiro Makimura, MD,* Masahiro Fukuoka, MD, PhD,† and Kazuhiko Nakagawa, MD, PhD**

A 62-year-old woman with an 18-pack-year history of smoking was found to have a solitary spiculated lesion in the right upper lung lobe and multiple pulmonary nodules on a computed tomography (CT) scan of the chest. A transcutaneous CT-guided needle biopsy specimen of the lung revealed adenocarcinoma. She received four cycles of chemotherapy with docetaxel and cisplatin, after which CT revealed marked tumor shrinkage. During follow-up for 3 months, progressive disease was diagnosed on the basis of the presence of an enhancement of cortical sulci on a CT scan of the brain. Mutation analysis of the lung cancer specimen showed the presence of an exon-19 deletion in the *epidermal growth factor receptor* (*EGFR*) gene, and gefitinib was administered orally at a dose of 250 mg once daily (Figure 1*A*). After 24 days of gefitinib, the patient manifested acutely deteriorating dyspnea with fever and cough. A chest CT scan revealed extensive bilateral ground-glass opacities throughout both lungs (Figure 1*B*). The results of sputum culture of bacteria or fungi and general blood tests, including those for fungal antigen and cytomegalovirus antigen, were negative. The patient had no prior interstitial lung disease (ILD) or preexisting collagen-vascular disease. Therefore, we concluded that the clinical course and imaging results were consistent with gefitinib-induced ILD. Gefitinib therapy was discontinued, and the treatment with high-dose methylprednisolone was initiated. Given that her symptoms and radiologic findings of gefitinib-induced ILD improved, the patient was discharged 14 days after discontinuation of gefitinib. As a result of progression of brain metastasis soon after discontinuation of gefitinib, whole-brain radiation therapy was delivered. Three months after discontinuation of gefitinib, the patient again experienced neurologic progression because of the brain metastasis, and the development of symptomatic brain metastasis was considered to be a contraindication for treatment with cytotoxic agents. After receiving full informed consent for the risk of recurrent ILD and high mortality rate after the onset of ILD, we administered erlotinib at a dose of 150 mg/d (Figure 1*C*). Nine weeks after the initiation of erlotinib treatment, a chest CT scan revealed no evidence of ILD and a reduction in the size of multiple pulmonary metastatic nodules (Figure 1*D*). After 11 weeks of erlotinib treatment, she developed meningeal carcinomatosis with progressive neurologic symptoms and discontinued erlotinib treatment. ILD has not been identified during the course of treatment with erlotinib.

DISCUSSION

Gefitinib-induced ILD is the most problematic toxicity, with an incidence reported to be approximately 4% in Japan and with about one third of the cases being fatal.[1] The predictive risk factors for ILD development include male sex, smoking, and the existence of pulmonary fibrosis. The discovery of somatic mutations in the tyrosine kinase domain of *EGFR* and of the association of such mutations with a high response rate to EGFR tyrosine kinase inhibitors (EGFR-TKIs) such as gefitinib and erlotinib has had a profound impact on the treatment of advanced non-small cell lung cancer. Gefitinib-induced severe ILD has been reported only rarely in *EGFR* mutation-positive patients, although the prevalence of EGFR mutations is estimated to be low in patients with risk factors for ILD.[2]

The mechanism of gefitinib-induced ILD has not been fully elucidated. The previous findings suggest that inhibition of EGFR-mediated signaling by gefitinib impairs the repair of and thereby exacerbates lung injury.[3–5] In the present case, the patient received oral erlotinib (150 mg) daily, which results in a steady-state plasma trough concentration, that is approximately 3.5 times that for gefitinib (250 mg), and tumor shrinkage was observed with no evidence of ILD. These observations suggest that blockade of the EGFR signaling pathway by EGFR-TKIs is not necessarily associated with the incidence of drug-related ILD. Erlotinib and gefitinib share a 4-anilinoquinazoline base structure but differ in the substituents attached to the quinazoline and anilino rings. Minor differences in

*Department of Medical Oncology, Kinki University School of Medicine, Osaka-Sayama; and †Department of Medical Oncology, Kinki University School of Medicine, Sakai Hospital, Minami-ku, Sakai, Osaka, Japan.

Disclosure: The authors declare no conflicts of interest.

Address for correspondence: Isamu Okamoto, MD, PhD, Department of Medical Oncology, Kinki University School of Medicine, 377-2 Ohno-higashi, Osaka-Sayama, Osaka 589-8511, Japan. E-mail: chiokamoto@dotd.med.kindai.ac.jp

ISSN: 1556-0864/10/0507-1103

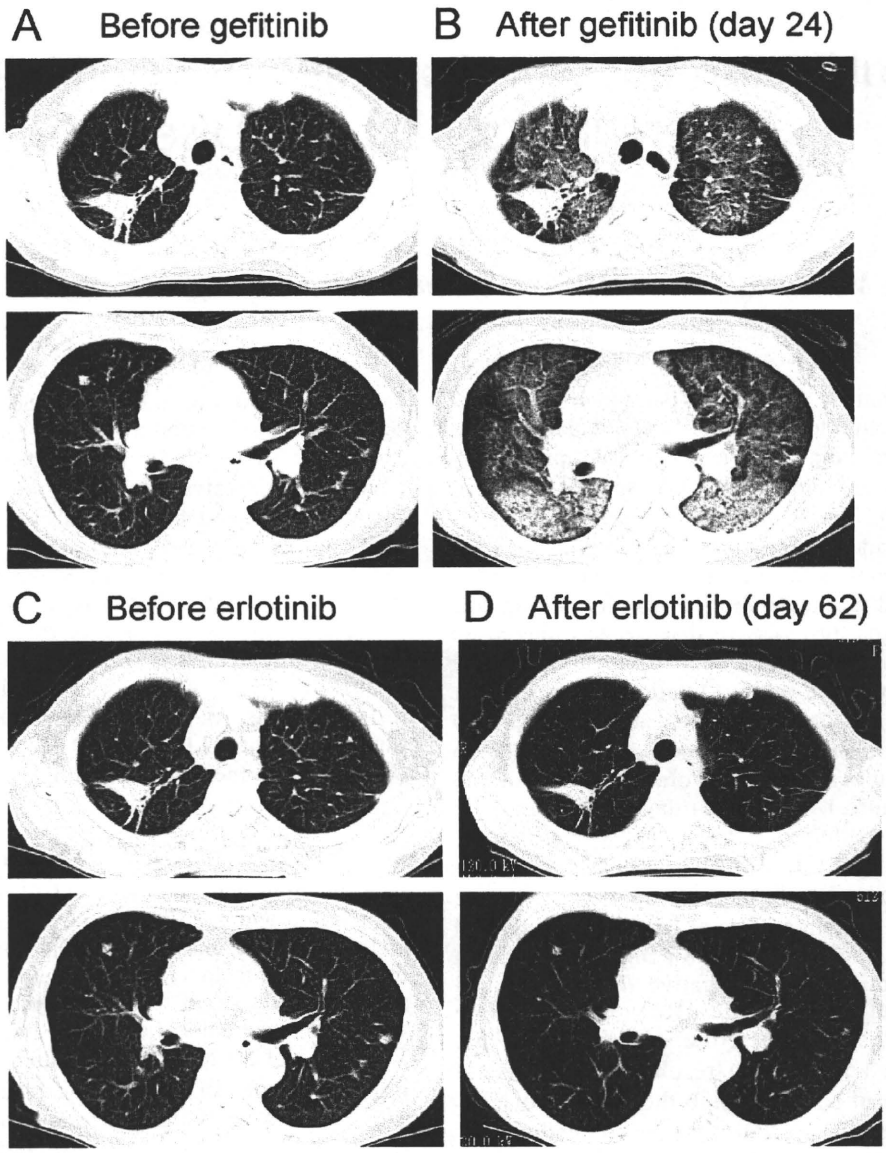

FIGURE 1. Chest computed tomography (CT) scans of the patient before (*A*) and 24 days after initiation of treatment with gefitinib (*B*). Bilateral pulmonary infiltrates on the chest CT were apparent on day 24 of gefitinib administration (*B*). After improvement of gefitinib-induced ILD, chest CT scans demonstrated that no ILD was observed in the patients receiving erlotinib (*C* and *D*).

the chemical structure of these compounds may, thus, influence lung toxicity.

We could successfully manage the patient who had once developed gefitinib-induced ILD with a full dose of erlotinib. The present case demonstrated that erlotinib may be one of the treatment options in such patients when alternative therapeutic options are limited. Because EGFR TKI-induced ILD has a high associated mortality, a careful assessment of clinical symptoms and radiographic findings and informed consent are needed in this setting.

REFERENCES

1. Ando M, Okamoto I, Yamamoto N, et al. Predictive factors for interstitial lung disease, antitumor response, and survival in non-small-cell lung cancer patients treated with gefitinib. *J Clin Oncol* 2006;24:2549–2556.
2. Tamura K, Okamoto I, Kashii T, et al. Multicentre prospective phase II trial of gefitinib for advanced non-small cell lung cancer with epidermal growth factor receptor mutations: results of the West Japan Thoracic Oncology Group trial (WJTOG0403). *Br J Cancer* 2008;98:907–914.
3. Hardie WD, Prows DR, Leikauf GD, et al. Attenuation of acute lung injury in transgenic mice expressing human transforming growth factor-alpha. *Am J Physiol* 1999;277:L1045–L1050.
4. Hardie WD, Prows DR, Piljan-Gentle A, et al. Dose-related protection from nickel-induced lung injury in transgenic mice expressing human transforming growth factor-alpha. *Am J Respir Cell Mol Biol* 2002;26:430–437.
5. Suzuki H, Aoshiba K, Yokohori N, et al. Epidermal growth factor receptor tyrosine kinase inhibition augments a murine model of pulmonary fibrosis. *Cancer Res* 2003;63:5054–5059.

Research Article

Molecular Cancer Therapeutics

Enhanced Anticancer Effect of the Combination of BIBW2992 and Thymidylate Synthase–Targeted Agents in Non–Small Cell Lung Cancer with the T790M Mutation of Epidermal Growth Factor Receptor

Ken Takezawa[1], Isamu Okamoto[1], Junko Tanizaki[1], Kiyoko Kuwata[1], Haruka Yamaguchi[1], Masahiro Fukuoka[3], Kazuto Nishio[2], and Kazuhiko Nakagawa[1]

Abstract

Most non–small cell lung cancer (NSCLC) tumors with activating mutations of the epidermal growth factor receptor (EGFR) are initially responsive to first-generation, reversible EGFR tyrosine kinase inhibitors (TKI) such as gefitinib, but they subsequently develop resistance to these drugs through either acquisition of an additional T790M mutation of EGFR or amplification of the proto-oncogene *MET*. We have now investigated the effects of combination treatment with thymidylate synthase (TS)–targeting drugs and the second-generation, irreversible EGFR-TKI BIBW2992 on the growth of NSCLC cells with the T790M mutation. The effects of BIBW2992 on EGFR signaling and TS expression in gefitinib-resistant NSCLC cells were examined by immunoblot analysis. The effects of BIBW2992 and the TS-targeting agents S-1 (or 5-fluorouracil) or pemetrexed on the growth of gefitinib-resistant NSCLC cells were examined both *in vitro* and *in vivo*. The combination of BIBW2992 with 5-fluorouracil or pemetrexed synergistically inhibited the proliferation of NSCLC cells with the T790M mutation *in vitro*, whereas an antagonistic interaction was apparent in this regard between gefitinib and either of these TS-targeting agents. BIBW2992 induced downregulation of TS in the gefitinib-resistant NSCLC cells, implicating depletion of TS in the enhanced antitumor effect of the combination therapy. The combination of BIBW2992 and either the oral fluoropyrimidine S-1 or pemetrexed also inhibited the growth of NSCLC xenografts with the T790M mutation to an extent greater than that apparent with either agent alone. The addition of TS-targeting drugs to BIBW2992 is a promising strategy to overcome EGFR-TKI resistance in NSCLC with the T790M mutation of EGFR. *Mol Cancer Ther; 9(6); 1647–56. ©2010 AACR.*

Introduction

Somatic mutations of the *epidermal growth factor receptor* (*EGFR*) gene are associated with a therapeutic response to EGFR tyrosine kinase inhibitors (TKI) in individuals with non–small cell lung cancer (NSCLC; 1–3). However, most such patients ultimately develop resistance to these drugs. Among patients with NSCLC who develop resistance to the first-generation EGFR-TKIs gefitinib or erlotinib, ~50% have tumors with a secondary T790M mutation in exon 20 of *EGFR* and ~20% have tumors that manifest amplification of the proto-oncogene *MET* (4–6). The identification of strategies or agents capable of overcoming acquired resistance to EGFR-TKIs is thus an important clinical goal.

Gefitinib and erlotinib act as ATP mimetics and reversible inhibitors at the tyrosine kinase domain of EGFR. In contrast, second-generation, irreversible EGFR-TKIs not only act as ATP mimetics but also covalently bind to Cys^{797} of EGFR, which allows them to inhibit EGFR phosphorylation even in the presence of a T790M secondary mutation. Irreversible EGFR-TKIs including BIBW2992 have been found to be effective in inhibiting the growth of NSCLC cells with the T790M mutation of EGFR both *in vitro* and *in vivo* (7–9). On the basis of these preclinical evaluations, various clinical trials are currently under way to determine the efficacy of these drugs in NSCLC patients.

S-1 is an oral fluoropyrimidine derivative that is also currently under evaluation for the treatment of NSCLC as a thymidylate synthase (TS)–targeted agent (10–12). A new antifolate drug, pemetrexed, has also been shown to inhibit tumor growth by targeting TS and is widely used in clinical settings (13, 14). We have previously shown that gefitinib-induced downregulation of TS and E2F1, a transcription factor that regulates expression of

Authors' Affiliations: Departments of [1]Medical Oncology and [2]Genome Biology, Kinki University School of Medicine; [3]Department of Medical Oncology, Kinki University School of Medicine, Sakai Hospital, Osaka, Japan

Note: Supplementary material for this article is available at Molecular Cancer Therapeutics Online (http://mct.aacrjournals.org/).

Corresponding Author: Isamu Okamoto, Department of Medical Oncology, Kinki University School of Medicine, 377-2 Ohno-higashi, Osaka-Sayama, Osaka 589-8511, Japan. Phone: 81-72-366-0221; Fax: 81-72-360-5000. E-mail: chi-okamoto@dotd.med.kindai.ac.jp

doi: 10.1158/1535-7163.MCT-09-1009

Table 1. IC_{50} values of BIBW2992 and gefitinib for inhibition of the growth of NSCLC cells *in vitro*

Cell line	IC_{50} (μmol/L)	
	BIBW2992	Gefitinib
	T790M (–)	
PC9	<0.001	0.031
HCC827	<0.001	0.011
	T790M (+)	
PC9/ZD	0.41	>5
H1975	0.22	>5

NOTE: Data are means of triplicates from representative experiments repeated a total of three times.

the TS gene, is responsible for the enhanced antitumor effect of combined treatment with S-1 (15, 16). However, an enhanced antitumor effect of this combination therapy on the growth of NSCLC cells harboring the T790M mutation of EGFR was not apparent as a result of continuous activation of EGFR and sustained expression of TS during gefitinib exposure. We have now investigated the potential efficacy of combined therapy with an irreversible EGFR-TKI and TS-targeted agents for the treatment of NSCLC with the T790M mutation of EGFR.

Materials and Methods

Cell culture and reagents

The human NSCLC cell lines PC9, PC9/ZD, HCC827, and NCI-H1975 (H1975) were obtained as described previously (16–18). All cells were cultured under a humidified atmosphere of 5% CO_2 at 37°C in RPMI 1640 (Sigma) supplemented with 10% fetal bovine serum. BIBW2992 was kindly provided by Boehringer Ingelheim Pharma; gefitinib was obtained from AstraZeneca; and 5-fluorouracil (5-FU), S-1, and pemetrexed were from Wako. U0126 and LY294002 were obtained from Cell Signaling Technology.

Growth inhibition assay *in vitro*

Cells were plated in 96-well flat-bottomed plates and cultured for 24 hours before exposure to various concentrations of drugs for 72 hours. TetraColor One (5 mmol/L tetrazolium monosodium salt and 0.2 mmol/L 1-methoxy-5-methyl phenazinium methylsulfate; Seikagaku) was then added to each well, and the cells were incubated for 3 hours at 37°C before measurement of absorbance at 490 nm with a Multiskan Spectrum instrument (Thermo Labsystems). Absorbance values were expressed as a percentage of that for untreated cells, and the concentration of tested drugs resulting in 50% growth inhibition (IC_{50}) was calculated. Data were analyzed by the median-effect method (CalcuSyn software, Biosoft) to determine the combination index (CI), a well-established index of the interaction between two drugs (19). CI values of <1, 1, and >1 indicate synergistic, additive, and antagonistic effects, respectively.

Immunoblot analysis

Cells were washed twice with ice-cold PBS and then lysed in a solution containing 20 mmol/L Tris-HCl (pH 7.5), 150 mmol/L NaCl, 1 mmol/L EDTA, 1% Triton X-100, 2.5 mmol/L sodium pyrophosphate, 1 mmol/L phenylmethylsulfonyl fluoride, and leupeptin (1 μg/mL). The protein concentration of cell lysates was determined with the Bradford reagent (Bio-Rad), and equal amounts of protein were subjected to SDS-PAGE on a 7.5% gel. The separated proteins were transferred to a nitrocellulose membrane, which was then exposed to 5% nonfat dried milk in PBS for 1 hour at room temperature before incubation overnight at 4°C with rabbit polyclonal antibodies to human phosphorylated EGFR (pY1068, 1:1,000 dilution; Cell Signaling Technology), phosphorylated AKT (1:1,000 dilution; Cell Signaling Technology), AKT (1:1,000 dilution; Cell Signaling Technology), phosphorylated extracellular signal-regulated kinase (ERK; 1:1,000 dilution; Santa Cruz Biotechnology), ERK (1:1,000 dilution; Santa Cruz Biotechnology), E2F1 (1:1,000 dilution; Santa Cruz Biotechnology), TS (1:1,000 dilution; Santa Cruz Biotechnology), or β-actin (1:500 dilution; Sigma) or with mouse monoclonal antibodies to EGFR (1:1,000 dilution; Zymed). The membrane was then washed with PBS containing 0.05% Tween 20 before incubation for 1 hour at room temperature with horseradish peroxidase–conjugated goat antibodies to rabbit (Sigma) or mouse (Santa Cruz Biotechnology) immunoglobulin G. Immune complexes were finally detected with chemiluminescence reagents (Perkin-Elmer Life Science).

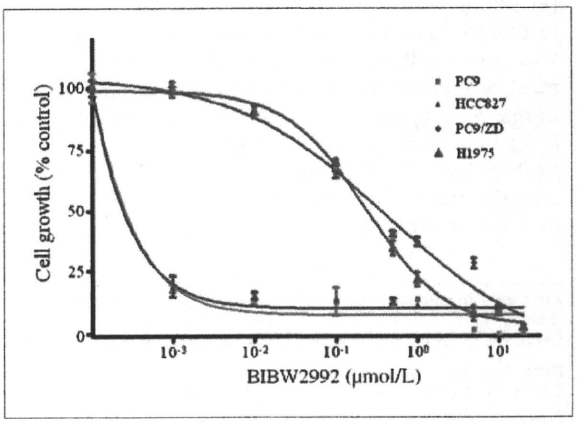

Figure 1. Effect of BIBW2992 on the growth of NSCLC cell lines *in vitro*. The indicated NSCLC cell lines were cultured for 72 h in complete medium containing various concentrations of BIBW2992, after which cell viability was assessed as described in Materials and Methods. Points, mean of triplicates from experiments that were repeated a total of three times with similar results; bars, SD.

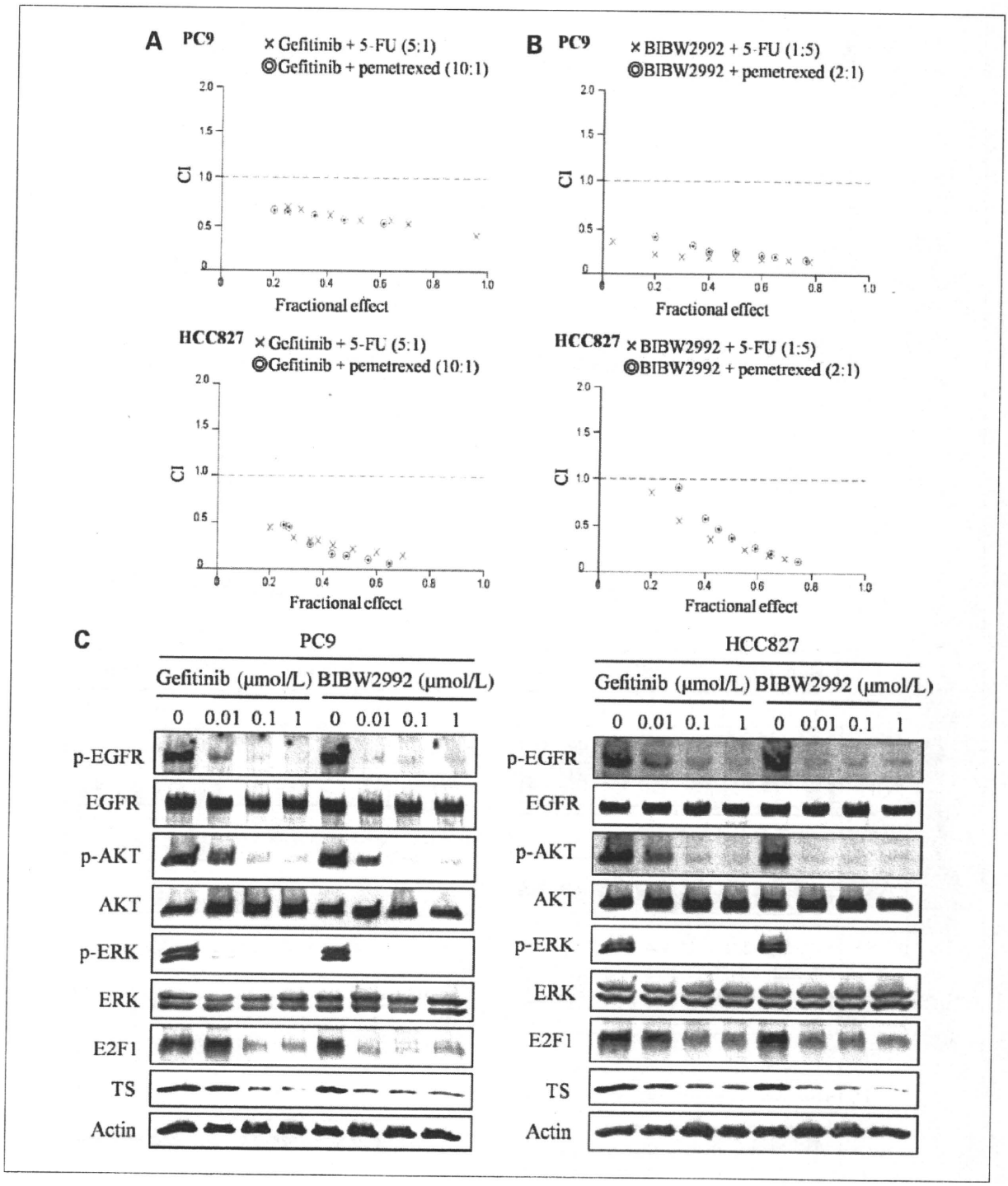

Figure 2. Effects of the combination of TS inhibitors (5-FU or pemetrexed) with EGFR-TKIs (gefitinib or BIBW2992) on the growth of gefitinib-sensitive NSCLC cell lines *in vitro*. A and B, sensitizing *EGFR* mutation-positive NSCLC (PC9 and HCC827) cells were incubated for 72 h with gefitinib (A) or BIBW2992 (B) together with 5-FU or pemetrexed at the indicated molar concentration ratios, after which cell viability was measured. The interaction between the two drugs in each combination was evaluated on the basis of the CI, which is plotted against fractional growth inhibition. Data are means of triplicates from experiments that were repeated a total of three times with similar results. C, cells were incubated for 24 h with gefitinib or BIBW2992 at the indicated concentrations in complete medium, after which cell lysates were prepared and subjected to immunoblot analysis with antibodies to phosphorylated (p) or total forms of EGFR, AKT, or ERK as well as with those to E2F1, TS, or β-actin (loading control).

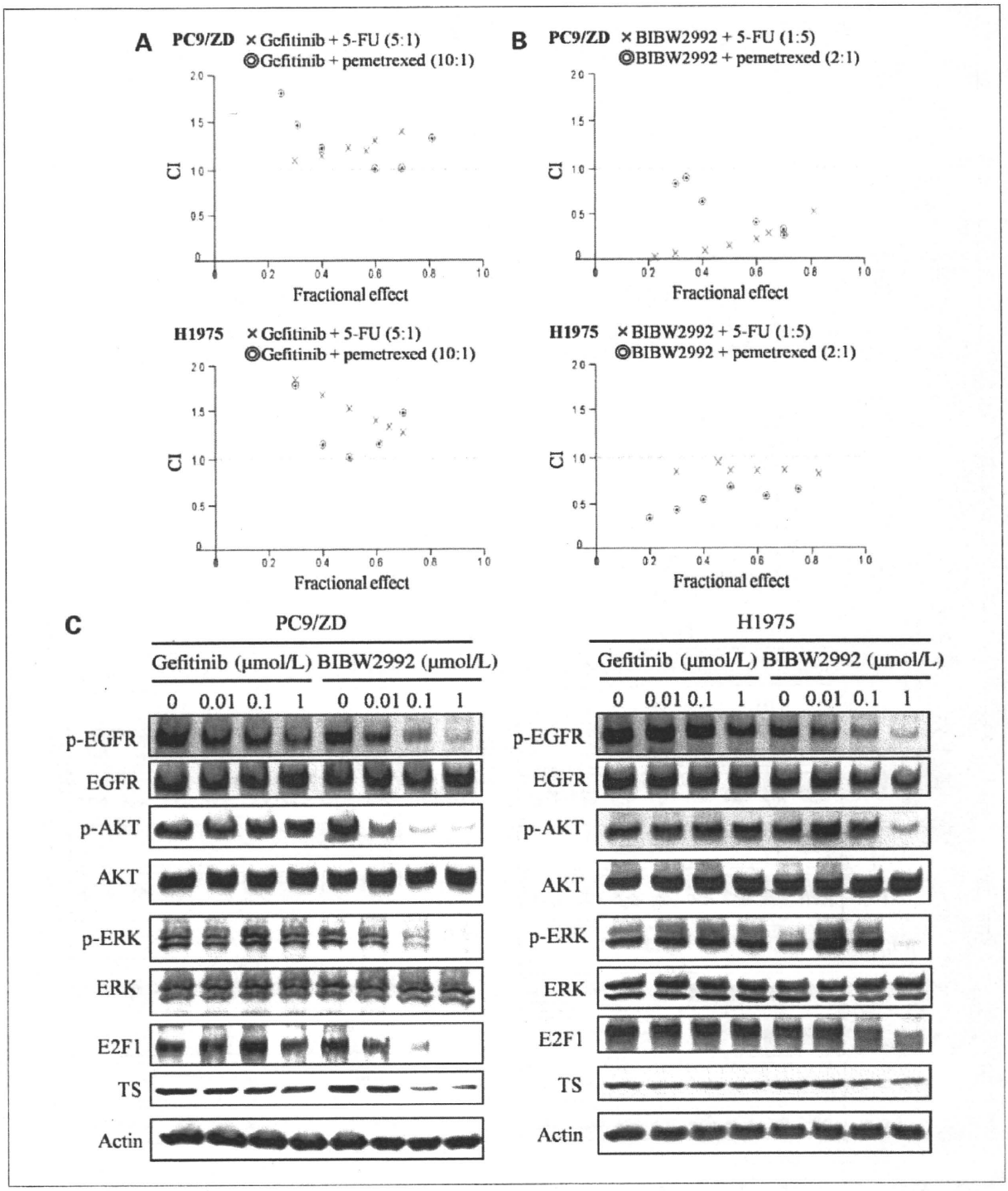

Figure 3. Effects of the combination of TS inhibitors (5-FU or pemetrexed) with EGFR-TKIs (gefitinib or BIBW2992) on the growth of gefitinib-resistant NSCLC cell lines *in vitro*. A and B, cells with a secondary T790M mutation of EGFR (PC9/ZD and H1975) were incubated for 72 h with gefitinib (A) or BIBW2992 (B) together with 5-FU or pemetrexed at the indicated molar concentration ratios, after which cell viability was measured and CI was plotted against fractional growth inhibition. Data are means of triplicates from experiments that were repeated a total of three times with similar results. C, cells were incubated for 24 h with gefitinib or BIBW2992 at the indicated concentrations in complete medium, after which cell lysates were prepared and subjected to immunoblot analysis as in Fig. 2C.